HHS Public Access

Author manuscript

Brain Res. Author manuscript; available in PMC 2023 September 11.

Published in final edited form as:

Brain Res. 2021 July 15; 1763: 147448. doi:10.1016/j.brainres.2021.147448.

Sex hormones regulate NHE1 functional expression and brain endothelial proteome to control paracellular integrity of the blood endothelial barrier

Kiera T. Blawn[a,1], **Kathryn L. Kellohen**[a,1], **Emily A. Galloway**[a], **Jared Wahl**[a], **Anjali Vivek**[a], **Vani G. Verkhovsky**[a], **Natalie K. Barker**[b], **Karissa E. Cottier**[a], **Tissiana G. Vallecillo**[a], **Paul R. Langlais**[b], **Erika Liktor-Busa**[a], **Todd W. Vanderah**[a], **Tally M. Largent-Milnes**[a,*]

[a]University of Arizona, Department of Pharmacology, Tucson, AZ, USA

[b]University of Arizona, Department of Medicine, Division of Endocrinology, College of Medicine, Tucson, AZ, USA

Abstract

Background: Sex hormones have been implicated in pH regulation of numerous physiological systems. One consistent factor of these studies is the sodium-hydrogen exchanger 1 (NHE1). NHE1 has been associated with pH homeostasis at epithelial barriers. Hormone fluctuations have been implicated in protection and risk for breaches in blood brain barrier (BBB)/blood endothelial barrier (BEB) integrity. Few studies, however, have investigated BBB/BEB integrity in neurological disorders in the context of sex-hormone regulation of pH homeostasis.

Methods//Results: Physiologically relevant concentrations of 17-β-estradiol (E2, 294 pM), progesterone (P, 100 nM), and testosterone (T,3.12 nM) were independently applied to cultured immortalized bEnd.3 brain endothelial cells to study the BEB. Individual gonadal hormones showed preferential effects on extracellular pH (E2), ^{14}C-sucrose uptake (T), stimulated paracellular breaches (P) with dependence on functional NHE1 expression without impacting transendothelial resistance (TEER) or total protein expression. While total NHE1 expression was not changed as determined via whole cell lysate and subcellular fractionation experiment,

*Corresponding author. tlargent@email.arizona.edu (T.M. Largent-Milnes).

[1]Co-first authors.

Authors Contributions

KTB, KLK, EAG, VGV, JW, NKB, KEC, TV, PRL, ELB, TWV, TML all contributed to the conception or design of the work. KTB, EAG, and KEC contributed to the harvest and analysis of CNS tissues from male and female rats. KLK, EAG, JW, AV, TV, and ELB contributed to the acquisition, analysis and/or interpretation of data collected from in vitro studies. JW and AV collected and analyzed TEER and extracellular pH. NKB, PRL, and TML collected, analyzed, and interpreted proteomics data. KTB, KLK, EAG, VGV, JW, ELB, and TML drafted and revised the work critically for important intellectual content. TML secured funding. All authors read and approved the final manuscript.

5.·Ethics approval and consent to participate

Not Applicable

6.·Consent for Publication

All Authors consent to the publication of the material presented

Declaration of Competing Interest

The authors declare that they have no known competing financial interests or personal relationships that could have appeared to influence the work reported in this paper.

Appendix A. Supplementary data

Supplementary data to this article can be found online at https://doi.org/10.1016/j.brainres.2021.147448.

biotinylation of NHE1 for surface membrane expression showed E2 reduced functional expression. Quantitative proteomic analysis revealed divergent effects of 17-β-estradiol and testosterone on changes in protein abundance in bEnd.3 endothelial cells as compared to untreated controls.

Conclusions: These data suggest that circulating levels of sex hormones may independently control BEB integrity by 1) regulating pH homeostasis through NHE1 functional expression and 2) modifying the endothelial proteome.

Keywords

Blood brain barrier; Endothelial; Hormones; pH; Proteome; Sodium-proton exchange

1. Introduction

Neuronal-glial excitability relies on an exquisite balance of ionic and metabolic composition of the extracellular and intracellular components of the central nervous system (CNS). Many CNS disorder events, including cortical spreading depression (CSD), stroke, traumatic brain injury (TBI), and epilepsy experience pH and ionic balance disruptions (Lauritzen et al., 2011; Zhao et al., 2016). For example, extracellular [K^+] increases to ~55 mM from 3 mM and [Na^+] falls to ~70 mM from 140 mM during CSD (Demaurex et al., 1995; Durham and Papapetropoulos, 2013; Haim et al., 2003; Lam et al., 2009; Rajkumar et al., 2001; Zohsel et al., 2006). This ionic imbalance is coupled to changes in metabolism (e.g., ATP, lactose) and intracellular homeostasis, such as intracellular and extracellular pH (Andrew et al., 2017; Ayata and Lauritzen, 2015; Basarsky et al., 1999; Brennan et al., 2007a, 2007b; Hartings et al., 2017; Lauritzen et al., 2011; Pietrobon and Moskowitz, 2014; Russo, 2015). In malignant hemispheric stroke, similar ionic changes are observed with the metabolic workload increasing to restore homeostasis as oxygen and glucose delivery is hindered by vessel constriction (Lauritzen et al., 2011). In TBI patients, reduced brain pH correlated with non-survival (Gupta et al., 2004). Epilepsy is triggered by pH imbalances as decreased intracellular pH in neurons can result in neuronal excitability (Zhao et al., 2016). Importantly, shifts in pH can modify properties of receptors, ion channels, enzymes and xenobiotics to enhance or dampen neural excitability and integrity of the BBB (Andrew et al., 2017; Hartings et al., 2017; Zhao et al., 2016).

The central nervous system (CNS) and CNS insults are influenced by sex hormones. Progesterone and estradiol demonstrate neuroprotective effects in preclinical models (Brinton, 2008; Brinton et al., 2008). Progesterone decreases brain swelling in animal models of TBI, exhibits anticonvulsant effects in an animal model of epilepsy, and induces neurogenesis in vitro in both rat cells and human cortical stem cells (Brinton et al., 2008). These various roles of progesterone emphasize its versatility and the neuroprotective effects within the brain that are still not well understood. Estradiol replacement after ovariectomy prevented the breakdown of the BBB induced by lipopolysaccharide (LPS) implicating estradiol as a neuroprotective agent in the initial stages of damage; this effect was lost at later timepoints after insult (Tomás-Camardiel et al., 2005). Moreover, female reproductive hormone fluctuations related to puberty, oral contraception, pregnancy, and menopause frequently coincide with the onset of or changes in migraine attacks (Hartings et al.,

2017; Zhao et al., 2016). Limited studies have investigated the effects of androgens as neuroprotective at the BBB. Thus, understanding the contributions of sex hormones to CNS homeostasis, including BBB function and pH regulation, is of high importance.

Sodium/hydrogen exchangers (NHEs) are surface membrane solute carriers that maintain intracellular pH by exchanging an intracellular proton at the expense of an extracellular Na^+ ion (Castañeda-Corral et al., 2012; Masereel et al., 2003; Putney et al., 2002). Sodium/hydrogen exchanger 1 (NHE1) is the most abundantly expressed sodium-proton exchanger in the CNS (Lam et al., 2009). Other NHEs have been implicated in CNS disorders; however, expression of NHE1 on endothelial cells is described as most critical. The dominant isoforms on rat blood brain barrier (BBB) endothelial cells are NHE1 and NHE2 (Lam et al., 2009). The studies herein determined the effects of sex hormones on the paracellular integrity of brain endothelial cell monolayers as a product of NHE1 expression and function to understand the contributions of sex to brain endothelial barrier (BEB) homeostasis. Sex hormone effects on the overall proteome of these brain endothelial cells was also determined to identify unique network effects of hormones on BEB maintenance.

2. Results

2.1. Cell surface expression of NHE1 is regulated by Progesterone and Testosterone

NHE1 is expressed on the plasma membrane of many cells, including brain endothelial cells. Using the immortalized bEnd.3 murine brain endothelial cell line, we assessed the total, subcellular compartment, and surface expression of NHE1 following 24 h incubation with E2, P, or T. While as determined by subcellular fraction did not show any effect of hormone exposure on NHE1 detection ($p = 0.28$ and $p < 0.60$, respectively), sustained exposure of murine brain endothelial cells to E2 significantly reduced surface expression of NHE1 as measured by biotinylated purification ($p = 0.049$; Fig. 1). In contrast, treatment with either P or T significantly increased detection of NHE1 on the plasma membrane (P, $p = 0.009$; T, $p = 0.009$). Finally, we assessed the total expression of NHE1 in whole cell lysates of bEnd.3 cells was hormone dose dependent on these immortalized cells; lowering the hormones concentrations did not change NHE1 total expression (Fig. 2). Together, these results suggest that P and T enhance NHE1 localization to the plasma membrane whereas E2 downregulates surface expression of NHE1 to selectively modulate biological functions of brain endothelial cells.

2.2. Testosterone regulates NHE1 to influence extracellular pH

Given that NHE1 surface expression is divergently regulated by P/T and E2 and that maintains intracellular pH, it stands to reason that changes in extracellular pH (pHe) will also be coupled to NHE1 function. We next evaluated the effects of 24 h hormone exposure with E2, P, and T to pHe (Fig. 3). Neither E2 nor P significantly changed pHe as compared to vehicle incubation. In contrast, T significantly increased pHe to 7.82 ± 0.05 over vehicle pHe = 7.68 ± 0.04; $p = 0.02$). Extracellular pH measurements were coupled to changes in the absorbance values of the media (Supplementary Fig. 1).

To investigate the role on NHE1 in the observed pHe, bEnd.3 cells were exposed to the hormones as above. Prior to measurement of pHe, the selective NHE1 antagonist, zoniporide, was added to the media (Fig. 3). Exposure to zoniporide did not significantly change pHe in cells incubated with vehicle ($p > 0.99$), E2 ($p = 0.09$), or P ($p > 0.99$). In endothelial cells exposed T, however, antagonism of NHE1 significantly reduced pHe as compared to T alone ($p = 0.003$). Together, these data indicate that T, but not E2 or P, increased pHe via NHE1-dependent mechanisms.

2.3. NHE1 plays a role in maintenance of brain endothelial monolayer paracellular integrity by testosterone and P, but not E2

Previously, loss of functional NHE1 has been linked to restoration of BBB paracellular integrity (Liktor-Busa et al., 2020). To determine if hormone-related changes in pHe can negatively influence the integrity of the BEB, we assessed monolayer junctional integrity using trans endothelial electrical resistance (TEER) and luminal to abluminal transport of ^{14}C-sucrose after hormone exposure as a measure of paracellular leak (Fig. 4). Initial studies revealed that TEER was unaltered under any condition as compared to vehicle (Fig. 4A). However, measurement of luminal to abluminal transport of ^{14}C-sucrose as a measure of basal paracellular integrity revealed that T, but not E2 or P reduced movement of ^{14}C-sucrose across the endothelial monolayer (Fig. 4B); this normalizes within 30 min and no differences were observed between individual hormone treatments (Fig. 4C). Thus, under basal conditions, testosterone tightens cell-to-cell junctions, but this is equalized over time.

To determine if observations in sucrose movement through the BEB monolayer reflected hormone-dependent changes in tight junction expression, we used Western blot to detect total expression of the anchoring protein zona occluding 1 (ZO-1) and the tight junction protein, claudin5 (Fig. 4D). 24 h exposure of immortalized bend.3 endothelial cells to sex hormones showed that claudin 5 detection was significantly higher after P ($p = 0.25$) and T ($p = 0.014$) exposure; ZO-1 detection was not influenced by hormones ($p = 0.73–0.94$ vs vehicle). Occludin was probed for but not detected by this techinique in this cell line under these conditions. These data indicate that hormone variability in paracellular integrity reflects changes int eh composition of tight junctions between endothelial cells.

We next assessed the paracellular integrity of bEnd.3 monolayers following a high potassium stimulus applied to the abluminal side after preexposure to hormones. As previously reported, KCl (60 mM, 5 min) significantly increased the amount of ^{14}C-sucrose detected on the abluminal side of the bEnd.3 monolayer (Fig. 5A). E2, P, and T pre-application all prevented this KCl mediated increased in ^{14}C-sucrose uptake suggesting a that the individual hormones at maximal physiological concentrations protect brain endothelial cells from paracellular breaches during K^+- mediated perturbations (Fig. 5B, C, D).

To evaluate if this hormone-mediated protection of the monolayer from K^+ stimulation was a result of NHE1 regulation, zoniporide (10 nM, 30 min) was added to the luminal side (Fig. 5A-D). Exposure to zoniporide did not influence ^{14}C-sucrose transport in cells treated with vehicle, E2, or T, the NHE1 blockers independent of stimulus applied (i. e., aCSF or KCl). Zoniporide significantly reduced ^{14}C-sucrose transport in cells pre-exposed to P

and stimulated with aCSF ($p = 0.02$) but not KCl ($p > 0.99$) suggesting that progesterone regulates paracellular permeability, in part, via NHE1. No differences were observed between groups at later time points (Fig. 5A'-D').

2.4. The bEnd.3 Endothelial cell proteome is differentially regulated by sex hormones

While hormones distinctly control NHE1 function and localization on bEnd.3 monolayers, it is possible that other proteins play a role in both monolayer integrity as well as pHe. We next used un-biased quantitative proteomics to determine the influence of hormone exposure on global protein expression levels in bEnd.3 cells (Fig. 6A). Using the reported peak serum concentrations during the rodent estrus cycle, cells were either vehicle-treated or incubated for 24 h in either E2 (294 pM) or T (3.12 nM) as the predominant sex hormones ($n = 4$/condition). Quantitative proteomic analysis comparing global protein expression changes between vehicle-treated controls and hormone treated cells identified 7120 total proteins across 72 fractions analyzed for the 12 biological samples. Unbiased principal component analysis (PCA) of the 805 significantly affected proteins from the 3-way ANOVA analysis revealed that the protein expression differences cluster together as either vehicle-treated, estrogen-treated, or testosterone-treated (Fig. 6B; Supplemental Table 1). We analyzed each hormone treatment solely versus the vehicle-treated control and discovered 229 (3.2%) proteins were significantly changed after estrogen treatment (Fig. 6C-D; Supplemental Tables 2–3) whereas testosterone exposure produced a much more robust effect at 871 (12.2%) affected proteins (Fig. 6E-F; Supplemental Tables 4–5). The effects of hormone treatment were distinct, as only 9% of the significantly affected proteins were shared between E2 and T (Fig. 6G; Supplemental Tables 6–7). Gene ontology (GO) enrichment analysis of the significantly affected proteins for each hormone treatment using the bioinformatic database DAVID (Huang da et al., 2009) was performed for GO-Molecular Function and GO-KEGG pathways, and the results are shown in Fig. 6H (Supplemental Tables 8–11).

2.5. Comparison of NHE1 and TJ expression between sexes in vivo.

To determine if these observations in immortalized murine brain endothelial cells were evident at a systems level, we assessed total NHE1, ZO1, occluding and claudin 5 expression in cortical samples from CD-1 mice (Fig. 7). Both NHE1, ZO-1, and occluding were detected in cortical brain samples in both male and female samples; claudin 5 detection was faint and not quantifiable without contrast enhancement. No statistically significant sex differences in whole tissue NHE1 were observed. However, ZO-1 was higher in females ($p = 0.048$) whereas occludin was higher in males ($p = 0.024$).

3. Discussion

NHE1 is a primary pH balancing protein that also regulates sodium ion concentration at epi- and endothelial cells, including those comprising the blood brain barrier/neurovascular unit (Lam et al., 2009). Sex hormones have been implicated in pH regulation by NHE1 of female reproductive organs (Gorodeski et al., 2005), cardio-protection during acidosis (Bupha-Intr et al., 2007), and osmoregulation. The purpose of the above study was to determine the influence of sex hormones on NHE1 expression and function on brain

endothelial cell monolayers to model the brain endothelial barrier (BEB). Our findings suggest that individual steroid hormones interact with NHE1 function to produce distinct outcomes on brain endothelial cells. Specifically, we found that while NHE1 expression was unchanged with the different sex hormones, localization, and functional differences in NHE1 were evident. Testosterone significantly reduced the uptake of ^{14}C-sucrose indicating a tightening of the paracellular junctions of the endothelial monolayer; this was supported by tight junction detection at higher levels than control. E2, but not P or T, regulated the extracellular pH and this was NHE1 dependent. Progesterone exposure led to reduced NHE1 function and limited endothelial monolayer paracellular permeability. These data suggest that sex hormones regulate functional expression of NHE1 to control paracellular permeability via tight junction control on brain endothelium.

3.1. NHE1, hormones, and BBB

BBB integrity is linked to hormone concentration (Atallah et al., 2017; Maggioli et al., 2016; Na et al., 2015) with emphasis on endothelial cells. These actions of steroid hormones on the BBB are attributed to ion dysregulation, oxidation state, inflammatory, and tight junction integrity and function. Testosterone depletion is associated with impaired BBB integrity and tight junction rearrangement and has been linked to barrier breaches in male MS patients(Atallah et al., 2017; Caruso et al., 2014). There is also evidence that excessive testosterone can lead to reductions in BBB integrity (Nierwińska et al., 2019). 17-β-estradiol, a testosterone metabolite and primary estrogen, is recognized as a neuroprotective steroid in vitro and in vivo by mitigating decreases in matrix metallo-proteases and TJ expression (Azcoitia et al., 2019; Na et al., 2015; Xiao et al., 2018). However, these beneficial effects of estrogens are lost with age in an ER-alpha receptor dependent manner (Kuruca et al., 2017). Studies of progesterone effects on the BBB indicate a clear neuroprotective effect in the setting of insult/injury(Hun Lee et al., 2015; Si et al., 2014), as does the active metabolite allopregnanolone (Ishrat et al., 2010, Limmroth et al., 1996).

During challenges at the BBB including hypoxia, mechanical stretch, hypertonicity, which cause an acidic pHe, NHE1 becomes active and induces cytoskeletal reorganization as a stress response for cell survival and protection (Putney et al., 2002; Song et al., 2018; Vallés et al., 2015; Zaun et al., 2012; Zhao et al., 2016). In turn, NHE1 mediated cytoskeletal reorganization regulates cell volume (Vallés et al., 2015) in endothelial as well as many other cell types (Amith et al., 2017; Bupha-Intr et al., 2007; Carraro-Lacroix et al., 2006; Chang et al., 2010; Chatterjee et al., 2014; Hendus-Altenburger et al., 2014; Putney et al., 2002; Qadri et al., 2014; Zhou and Baltz, 2013). Moreover, phosphorylation leads to increases in antiport activity of NHE1(Amith et al., 2017; Hendus-Altenburger et al., 2014; Nørholm et al., 2011). Hormones are reported to target serine and threonine rich sections of the full NHE1 protein (Vallés et al., 2015). To determine the role of hormone regulation of pH in these actions at the BEB, we assessed in vitro regulation of NHE1 in the presence of the individual hormones.

3.2. NHE1 and E2

Estrogen-mediated regulation of NHE1 transcription, translation, and activity has been reported in a number of tissues including uterus (Gholami et al., 2013), cardiac myocytes (Bupha-Intr et al., 2007; Kilic et al., 2009), some breast epithelium (Lin et al., 2007), intestines (Blaurock et al., 1995), immune cells (Singh et al., 2016), and hippocampus (Sárvári et al., 2016). These effects, including increased expression, have been attributed to direct actions at nuclear hormone receptors, the G-protein coupled receptor, GPR30, as well as thyroid hormone signaling (Blaurock et al., 1995; Bupha-Intr et al., 2007; Kilic et al., 2009; Lin et al., 2007; Singh et al., 2016). Presently, estradiol (294 pM) exposure significantly reduced the amount of NHE1 on the endothelial cell surface without changing total protein expression. These data align with those of Lam, which showed that 17-β-estradiol (1–100 nM) reduced NHE1 activity and may explain their observations with concentrations of estradiol >1 nM (Lam et al., 2009). However, this loss of cell surface NHE1 did not have significant functional impact on pH or paracellular integrity of endothelial monolayers. Indeed, E2 can inhibit arginine vasopressin stimulated activity of NHE1 (Na et al., 2015) as well as myofilament contractions mediated by NHE1 activity (Bupha-Intr et al., 2007) in vascular endothelial and smooth muscle cells. Thus, E2 regulation of NHE1 localization may have alternative biological implications for BEB/BBB protection.

3.3. NHE1 and P

Interactions between progesterone and NHE1 are documented in the endometrium and in T-cells (Wang et al., 2003) but not in cells comprising the vasculature. In the endometrium, 3 days of progesterone dosing to ovariectomized rats lowered intrauterine pH that was reversed by amiloride, a non-selective inhibitor that blocks NHE1 activity and increased the expression of NHE1 in the uterus (Naguib et al., 2011). Progesterone exerts non-genomic effects in T-cells by inhibiting NHE1 activity to suppress T cell mediated immunomodulation (Chang et al., 2010; Chien et al., 2007, 2016). However, this T-cell modulation has been suggested to be through a Ca^{++} dependent mechanism, rather than a direct action at NHE1 (Lai et al., 2012). In the present study, extended progesterone incubation (24 h) did not significantly reduce ^{14}C-sucrose uptake, a marker of paracellular permeability, across the endothelial cell monolayer alone. However, addition of the NHE1 inhibitor, zoniporide following exposure to progesterone did suppress sucrose uptake suggesting that NHE1 activity contributes to the progesterone-sensitive permeability of brain endothelium. Unlike the endometrium, this was not due to changes in NHE1 expression (Wang et al., 2003), but rather, to increased surface expression of NHE1 following progesterone exposure.

3.4. NHE1 and T

There have been limited investigations performed on the relationship between testosterone or the androgen receptor and NHE1. Chatterjee and colleagues suggested that albumin-conjugated testosterone rapidly increased intracellular pH of prostate cancer cells through androgen receptor activation of Rho/Rock signaling to increase NHE1 activity; this effect was lost after 24 h exposure (Chatterjee et al., 2014). Herein, we found that 24

h pretreatment with testosterone increased pHe as compared to vehicle in an NHE1 dependent manner; this may be attributed to the increase in cell surface NHE1 induced by testosterone as observed by Chatterjee. Testosterone exposure also reduced paracellular movement of ^{14}C-sucrose demonstrating a tightening of endothelial junctions under basal conditions. Therefore, testosterone-mediated regulation of NHE1 in brain endothelial cells may contribute to maintenance of BEB integrity.

3.5. Proteomic changes.

Recognizing that the observations of non-genomic regulation of NHE1 with E2 and P are not solitary outcomes, the genomic signaling of these hormones through their respective receptors in undeniable. Thus, it is possible that other NHEs (Beydoun et al., 2017; Damkier et al., 2018; Milosavljevic et al., 2014; O'Donnell, 2014; Prasad and Rao, 2015; Shi et al., 2013) or transporters contribute to the extracellular alkalosis of endothelial cells in these studies (Abbott et al., 2010; Lam et al., 2009, 2013; Lin et al., 2014; Putney et al., 2002; Turovsky et al., 2016; Yuen et al., 2018). Proteomic analysis using physiologically relevant concentrations of E2 and testosterone revealed that these hormones are associated with distinct and complex signatures of protein expression in brain endothelial cells. For example, E2 induced expression of proteins relevant to kinase activity with actions in chemokine signaling, phagosomes, and metabolic changes. These KEGG pathways are linked to regulation of immune cell modulation and inflammation cascades known to be influenced by estrogens (Plackett et al., 2016; Seillet et al., 2013). In contrast, testosterone enriched proteins relevant to cell–cell adhesion with identified KEGG pathways including VEGF signaling, lipid metabolism, and regulation of RNA transport and degradation. These data would suggest that sexual dimorphism in the proteome and network signaling of bEnd.3 cells that may contribute to the present observations including regulation of paracellular integrity of cells of the BEB.

3.6. In vivo findings

Sex differences in BBB integrity and molecular composition have been documented for multiple transporters under naive and insult conditions in several mouse strains and in rats (Brzica et al., 2018; Diler et al., 2007; Torres and Bynoe, 2017). Here, we describe in CD1 mice, that sex differences in NHE1 are not apparent at the whole tissue level, although variability in individual cell types may exist. However, in the same tissue samples, we found that ZO1 was higher in females but occludin was higher in males. Therefore, in this strain, female mice may be more susceptible to loss of BBB integrity by insults that target cytoskeletal reorganization. Conversely, male CD1 mice may be more protected by having a higher basal level of the junction spanning occludin. Additional experiments are required to confirm these possibilities.

3.7. Clinical relevance of findings

The Institute of Medicine recognizes that sex hormones play divergent roles in protection or susceptibility to neurological disorders including but not limited to migraine, multiple sclerosis, epilepsy and ischemic stroke (Avila et al., 2018; Schipper, 1986; The Lancet 2019; Wizemann and Pardue, 2001; Zárate et al., 2017) in brain region and cell-selective manners. In the current study, no statistical differences in NHE1 expression were observed between

male and female whole cortical samples (i.e., primary endothelial cells were not isolated). Thus, basal differences between the sexes may be absent but exacerbated by insult.

CSD events are associated most frequently with migraine with aura, but have been reported after ischemic stroke and traumatic brain injury as well as epilepsy and multiple sclerosis (Charles and Baca, 2013; Lauritzen et al., 2011; Sun et al., 2011). Differences in brain pH have been reported during CSD events (Cottier et al., 2018; Fried et al., 2018). All of these disorders have been 1) linked to changes in NHE1 function including gain of function and loss of function (Liktor-Busa et al., 2020) and 2) are linked to impaired BBB integrity (Chung et al., 2016; Cottier et al., 2018; Fried et al., 2018; Hind et al., 2016; Li et al., 2018; Liktor-Busa et al., 2020; O'Donnell, 2014; Wang et al., 2018; Yuen et al., 2018). Thus, the above observations may have high clinical importance in the development of these pathologies and in the ability to pharmaceutically mitigate them.

3.8. Limitations of this study

While these findings are novel and identify the individual contributions of sex hormones to brain endothelial cell pH homeostasis and monolayer integrity, full extrapolation to an intact system is impaired. First, study only investigated focused on brain endothelial cell expression of NHE1 for relevance to the BEB rather than the NVU. The cells used for this study are an immortalized brain endothelial cell line. Thus, studies using primary brain endothelial cells, stem-cell derived endothelial cells, or human donor brain endothelial are required to confirm our observations. Neurons were omitted given the high variability in neuron subclassifications within each region of the CNS and the potential that expression patterns would differ based on circuit integration. Astrocytic and microglial expression and regulation of NHE1 is reported (Song et al., 2018; Shi et al., 2011) but is activation dependent; thus selection of tissues to analyze is critical. Pericytes on the neurovascular unit may also express NHE1 which should be investigated. These important contributions are one factor that may account for our observations using tissue from male and female mice.

Second, studies above evaluated NHE1 expression, localization, and function using pharmacological approaches, activity differences by other means (i.e. H^+ flux, phosphorylation state) were not determined. Gain of NHE1 function is linked with increased phosphorylation of NHE1 (Luo et al., 2007; Qadri et al., 2014); thus, it is possible that sex hormones change NHE1 phosphorylation state and subsequently function. At the level of expression, individual nuclear hormone receptors (ESR1, ESR2, AR, PR-long, PR-short) have direct ties to regulation of NHE1 via gonadal response elements, though not determined here. It is also possible that some of the results represent indirect interaction; with hormone nuclear receptors associating with other transcription factor complexes (e.g., AP-1/c-Jun, c-Fos, ATF-2, Sp1, Sp3, NFkappa B, etc.; available from: https://www.uniprot.org/uniprot/P03372).

Finally, the studies above presented data collected using immortalized mouse lines in vitro. It is likely that species differences exist in how NHE1 is regulated by hormones and thus, use of human derived cells is critical to substantiate the clinical implications of the current findings. Moreover, the exact changes in the proteome induced by hormone exposure likely differ between species. Despite these limitations, sex hormones play a role in regulating

NHE1 to control the pH of the brain endothelial environment as well as cell function as a barrier. These results justify future investigation into the contributions of sex hormones to blood to CNS uptake of drugs and BBB structural integrity in disease.

3.9. Conclusion

Overall, E2, P, and T may influence BEB integrity by 1) regulating NHE1 expression, 2) regulating NHE1 function and therefore pH homeostasis, and 3) proteome manipulation to engage distinct molecular pathways. Together, these findings highlight the need for advanced understanding of hormone regulation of BEB integrity under physiological and pathological conditions in multiple models (e.g., primary cells, stem-cell derived cells, or in vivo) to determine how these changes in BBB permeability (Cottier et al., 2018) may impact therapeutic efficacy and underscore sex- responsivity to pharmaceutics (Jeong et al., 2008; Li et al., 2016; Mathew, 2011).

4. Experimental procedure

4.1. Drugs and Reagents

Protease and phosphatase inhibitor cocktails were purchased from BiMake. Pierce™ BCA Protein Assay Kit was purchased from ThermoScientific for cell protein quantification. Lysis sample buffer was prepared using chemicals purchased from Sigma-Aldrich (St. Louis, MO). DTT reducing agent was also purchased from Sigma-Aldrich (St. Louis, MO). Precision Plus dual color pre-stained molecular weight markers, and TGX criterion gels were purchased from Bio-Rad (Hercules, CA, USA).

4.2. Hormones

Physiological concentrations of 17-β-estradiol (Sigma-Aldrich E8875–5G), progesterone (Sigma-Aldrich P8783–1G), and testosterone (Sigma-Aldrich T1500) from cycling female rats were used to stimulate cells for 24 h (Haim et al., 2003; Rajkumar et al., 2001). Additionally, serum levels of hormones during rat pregnancy were simulated, as well as peak male rat levels of individual hormones. Concentrations of 17-β-estradiol (18 pM-440 pM) and testosterone (350 pM-3.12 nM) were prepared in media with 0.1% DMSO. Progesterone was reconstituted to a stock solution of 20 ug/mL using HPLC grade ethanol. Dilutions of progesterone were prepared (0.1–100 nM) using media for bEnd.3 endothelial cells or astrocytes. The vehicle was prepared using a dilution of 0.01% ethanol in media. Progesterone levels were used relevant to the estrous cycle, and a serial dilution of progesterone was performed using physiological references (Haim et al., 2003).

4.3. Cell Culture

bEND.3 cells were cultured in 75 cm^2 standard flasks. They were sustained with media comprised of DMEM (ThermoScientific), supplemented with 2 mM L-glutamine, 10% fetal bovine serum (ThermoScientific), and 1% pen/strep (ThermoScientific). C8-D1A cells were cultured in 75 cm^2 standard flasks. They were sustained with media comprised of DMEM (ThermoScientific), supplemented with 10% fetal bovine serum (ThermoScientific), and 1% pen/strep (ThermoScientific). All cell lines were cultured at 37 °C in a humidified 5% CO_2/95% air atmosphere.

4.4. Cell Treatment

Cells were plated onto 6 well plates and cultured in the presence of astrocyte conditioned media to ensure tightly joined monolayer formation, with the following concentrations of progesterone, 17-β-estradiol, and testosterone as calculated from cycling female rats (Haim et al., 2003; Rajkumar et al., 2001). While ACM is not a complete representation of the neurovascular milieu, it does ensure tight junction formation. Treatment was 24 h, then washed with 1X PBS

4.5. Western blot Analysis

Following treatment, cells were lysed with buffer containing 20 mM Tris-HCl (pH 7.4), 50 mM NaCl, 2 mM $MgCl_2$ hexahydrate, 1% (vol/vol) NP40, 0.5% (w/vol) sodium deoxycholate, 0.1% (w/vol) SDS supplemented with protease and phosphatase inhibitor cocktail (BiMake). Protein content was assessed using a BCA protein assay. 20 ug of total proteins were loaded on TGX precast gels. Western Blot Analysis was performed by loading the samples onto a 10% SDS polyacrylamide gel (Criterion™ TGX™ Precast Gels from Bio-Rad, Cat. # 5671033). The gels were run in Tris/Glycine/SDS buffer at 150 V for ten minutes followed by 190 V for 40 min. The gels were subsequently transferred to membranes (Bio-Rad Immun-Blot® PVDF Membrane for Protein Blotting, Cat. # 1620177) and then blocked in 5% BSA in Tris-buffered saline with Tween 20 (TBST) solution for one hour. NHE1 primary antibodies were prepared (5% BSA in a 1:1,000 dilution, Abcam Cat. # AB67313). After incubation in primary antibody, the membranes were washed three times with 10 min washes in TBST. Secondary antirabbit IgG, HRP-linked antibody was prepared (5% BSA in a 1:20,000 dilution, Cell Signaling Technology, Cat. # 7074S) and the membranes were blocked in secondary antibody for one hour and then washed three times with five-minute washes in TBST. The membranes were then immersed in ESL solution for five minutes (Clarity™ Western ECL Substrate from Bio-Rad, Cat. # 170–5061) and developed. The membranes were subsequently stripped (One Minute® Plus Western Blot Stripping Buffer from GM Biosciences, Cat. # GM6015) and incubated overnight in α-tubulin primary antibody (5% BSA in a 1:100,000 dilution, Cell Signaling Technology, Cat. # 3873S). The membranes were then washed three times with five-minute washes in TBST. Secondary anti-mouse IgG, HRP-linked antibody was prepared (5% BSA in a 1:40,000 dilution, Cell Signaling Technology, Cat # 7076S) and membranes blocked in secondary antibody for one hour. For cellular subfractionation analyses, 40 ug of protein was loaded per lane in 10% SDS Page running gel. NHE1 (5% BSA in a 1:500 dilution, Abcam Cat. # AB67313) was used, with the following used as loading controls for their respective cell fraction: α-Tubulin (5% BSA in a 1:20000 dilution, Abcam Cat# AB7291) cytoplasmic fraction, Lamin B (5% BSA in a 1:1000 dilution, Invitrogen Cat #PA5 19468) Nuclear fraction, PECAM/CD-31 (5% BSA in a 1:1000 dilution, Santa Cruz Cat# 376764). Secondary treatment same as above. Antibodies used for tight junction imaging in b.End3 cells were as follows: Claudin-5 (5% BSA in a 1:500 dilution, Invitrogen Cat# 35–2500), Zona Occludins-1 (5% BSA in a 1:500 dilution, Invitrogen Cat# 33–9100), α-Tubulin (5% BSA in a 1:20000 dilution, Abcam Cat# AB7291). Samples were loaded with 20 ug total protein per sample. For Naïve mouse whole brain lysate, 80 ug of protein was loaded per sample, with the same antibody concentrations stated above as well as occludin (5% BSA in a 1:500 dilution, Invitrogen Cat# 35–1500).

4.6. Biotinylation

Biotin buffer was prepared with 1x PBS and 2 mM CaCl, buffered to a pH of 7.2. NHS-SS Biotin reagent was used from the Thermo-Fisher cell surface isolation kit (Thermo, ref: 89881). Four six well tissue culture plates (Corning) were pretreated with a 20% collagen solution for two hours and then seeded with 50,000b.End3 cells per well (Passage 18), with 2 mL of astrocyte conditioned media (ACM) supplied per well for a growth medium. At confluence, cells were exposed for 24 h to 1) Vehicle (ACM), 2) Estradiol (E_2) 294 pM in ACM, 3) Progesterone (P), 100 nM in ACM, and 4) Testosterone (T) 3.12 nM in ACM (37 °C with 5% CO_2). Hormone treatments were then removed, and cell plates were chilled to 4 °C and rinsed in 1x PBS buffered to pH 8.0. 1 mL of pre prepared biotin buffer containing NHS-SS biotin linking reagent (Thermo) was then added to each well and then incubated at 4 °C for 25 min, after which a fresh aliquot of biotin buffer was added and cells were incubated at 4 °C for another 25 min. After incubation, biotin buffer was removed and cells were washed 3 times with 1x PBS, pH of 8.0. Cell lysis buffer was prepared with protease and phosphatase inhibitors, added to lysis buffer at a ratio of 1:100. 1 mL of lysis preparation was added to each well of the four plates. Cells and lysis buffer were harvested and transferred to a 1.5 mL microfuge tube and incubated on ice for 1 h prior to centrifugation at 14,000 RPM for 10 min at 4 °C; supernatant was decanted and collected. Neutravidin (Thermo) was then equilibrated in lysis buffer by adding 1800 μL of the 50% Neutravidin-agarose slurry to a 2 mL centrifuge tube and centrifuging at 14,000 RPM for 10 min at 4 °C and resuspended in 1800 μL lysis buffer. Resuspended Neutravidin was then added to each sample at 150 μL Neutravidin suspension per well and incubated overnight at 4 °C on a rocker. Samples were re-aliquoted and centrifuged at 14,000 RPM for 5 s to pellet Neutravidin beads. After removing supernatant, Neutravidin pellets were washed three times with 500 μL lysis buffer, twice with 500 μL high salt buffer, and once with 500 μL no salt buffer; all washes lasted for three min. After washes, pellets were eluted into 60 μL 2x SDS sample buffer with 10% DTT. Samples were heated to 95 °C for 10 min on a heat block, cooled to RT, and loaded onto a 10% SDS PAGE gel, run for 40 min at 190 V, then transferred to a nitrocellulose membrane (1 h at 20 V). The membrane was blocked in 5% milk in TBST overnight at 4 °C then incubated with anti-NHE1 antibody (1:500, Invitrogen) in 5% TBST overnight at 4 °C on a rocker. The membrane was treated with anti-rabbit fluorescent secondary antibody (1:10000, LiCor) in 5% TBST, for 1 h at room temperature. Imaging was performed as described above

4.7. Cellular subfractionation

b.END3 endothelial cells were sub-cultured 15 times in T75 cell culture flasks and allowed to grow to confluency. Upon reaching confluency, cells were harvested via trypsinization with 0.025% trypsin-EDTA (Gibco). After harvesting cells were quantified for total and live cell count with trypan blue staining, cells were then seeded on 4 6 well plates (Corning) and seeded at an initial count of 50,000 cells per well, volume was then brought up to 2 mL with DMEM media (Gibco) with 5% FBS, 2 mM L Glutamine, and 2 mM Penicillin/Streptomycin added to media during preparation. Cells were then incubated at 37 °C with 5% CO_2 with DMEM media (Gibco) and allowed to grow until full confluence was observed microscopically. Upon reaching confluence, media was removed and replaced with astrocyte conditioned media (ACM, prepared in house) and allowed to incubate overnight

at 37 °C 5% CO_2. Following incubation, each plate was relegated to either a control group (Vehicle) or one of three treatment groups consisting of 1) 214 pM Estradiol, 2) 100 nM Progesterone, and 4) 3.14 nM Testosterone, ACM used as a vehicle for each treatment. Each well received 2 mL of its respected treatment and were incubated for 24 h at 37 °C with 5% CO_2. Cells were then harvested with 0.025% Trypsin-EDTA and pelleted by centrifugation at 500*g* for 5 min, after which supernatant was decanted and cell pellets were resuspended in 1x PBS. Cell suspensions were then pooled according to treatment group, transferred to a microfuge tube, and centrifuged at 500*g* for 3 min. Supernatant was then decanted, with pellets kept dry for subcellular fractionation. Subcellular fractionation was then carried out utilizing Thermo scientific subcellular fractionation kit (catalog #78840), fractioning cells into three compartments, cytoplasm, membrane, and nuclear fractions. Stock buffers from sub fractionation kit for each fraction were prepared by addition of protease and phosphatase inhibitors at a ratio of 1:100 and placed on ice. Cell pellets for each treatment group were resuspended in 200 μL cytoplasmic extraction buffer (CEB), then incubated at 4 °C for 10 min on mixing platform. Suspensions were then centrifuged at 500*g* for 5 min, with supernatant containing cytoplasmic fraction transferred to a new tube, separated by treatment group and placed on ice. Cell pellets for each treatment group were then resuspended in 200 μL of membrane extraction buffer (MEB), vortexed, and incubated at 4 °C for 10 min on a rocking platform. Suspension was then centrifuged at 3000*g* for 5 min with supernatant containing membrane fraction transferred to new tube, separated by treatment, and placed on ice. Cell pellet was then resuspended in 100 μL nuclear extraction buffer (NEB), vortexed, and incubated at 4 °C for 30 min on a rocking platform. Tubes were then centrifuged at 5000*g* for 5 min, with the supernatant containing the nuclear fraction decanted into a new tube, separated by treatment and placed on ice, with the cell pellets being discarded. After collection of cell fractions, protein concentration was determined using a colorimetric BSA protein assay and frozen for Western blot imaging.

4.8. Trans-Endothelial electrical resistance (TEER)

bEnd.3 mouse endothelial cells were cultured on collagen coated *trans*-well inserts (Corning) with 500 μL bEnd.3 media for growth facilitation at 37 °C incubation. Abluminal side wells were treated with 1000 μL astrocyte conditioned media (ACM) at point of cell seeding to create an in vitro model of the BBB. ACM was prepared by incubating confluent CD18A astrocytes with Gibco DMEM media with 10% FBS and 1% penicillin–streptomycin and incubated for 24 h at 37 °C. bEnd.3 cells cultured on luminal side of *trans*-well insert were then treated with media (naïve group), 294 pM E2 (17-beta-estradiol group), 3.12 nM T (Testosterone group) or 1 nM P (Progesterone group). Hormones were diluted into bEnd.3 DMEM media then aliquoted in 500 μL aliquots for each respective treatment group on the luminal side of the *trans*-well plate. After 24 h incubation the hormone treated media was removed and replaced with fresh bEnd.3 DMEM media. Once the fresh media was added a baseline TEER measurement was taken via chopstick method (EVOM2). Trans endothelial electrical resistance (TEER) was then measured with chopstick electrodes (EVOM2) at the following timepoints: Baseline (pre hormone), 0 min (24 h post-hormone) and at 10, 20, 30, 60, 120, 180, and 360 min after removal of hormone. All measurements were repeated in triplicate via use of three, 12-well *trans*-well trays (Corning).

4.9. pH measures

Extracellular pH was measured before and after hormone treatment using FiveEasy Plus pH meter FP20 (Mettler Toledo) with Micro pH electrode LE422 in triplicate over three separate experiments.

4.10. Sucrose transport Assay

bEnd.3 cells were seeded 6.0×10^4 cells/cm^2 on the luminal side of collagen-coated filter membranes (0.4 μm pore polyester membrane) of 24-well tissue culture inserts (Costar, 3470). The cell culture inserts were incubated at 37 °C (5% CO_2) for 4–5 days. One day before experiment, astrocyte (C8-D1A cells)-conditioned media was added to the abluminal side of the inserts and incubated overnight at 37 °C (5% CO_2, humidified). ^{14}C-sucrose (PerkinElmer, NEC100XOO1MC) was applied to the luminal side to monitor the paracellular uptake at 0.25 μCi/ml concentration 24 h after hormone application to the luminal side and collected after 5 min and 30 min (relative to sucrose). The radioactivity of samples from the abluminal side was measured for disintegrations per minute (dpm; 1450 LSC and Luminescence Counter; PerkinElmer). For each individual experiment, 3–4 inserts/group with cells and three inserts without cells were assayed. The radioactivity in the inserts without cells at both time-points were two–three times higher compared to the inserts with cells, indicating the existence of barrier.

4.11. Proteomics

In-gel Digestion.—To determine changes in the global bEnd.3 cell proteome upon sex hormone treatment, bEnd.3 cells were either vehicle-treated or treated with 294 pM E2 or 3.12 nM T (n = 4 each). bEnd.3 cell lysates were prepared as for the Western blot (methods above). 200 μg of the bEnd.3 cell lysate supernatant was separated on a 10% SDS-PAGE gel and stained with Bio-Safe Coomassie G-250 Stain. Each lane of the SDS-PAGE gel was cut into six slices. The gel slices were subjected to trypsin digestion and the resulting peptides were purified by C18-based desalting exactly as previously described (Kruse et al., 2017; Parker et al., 2019).

Mass spectrometry and Database Search.—HPLC-ESI-MS/MS was performed in positive ion mode on a Thermo Scientific Orbitrap Fusion Lumos tribrid mass spectrometer fitted with an EASY-Spray Source (Thermo Scientific, San Jose, CA). NanoLC was performed exactly as previously described (Kruse et al., 2017; Parker et al., 2019). Tandem mass spectra were extracted from Xcalibur ‘RAW’ files and charge states were assigned using the ProteoWizard 3.0 msConvert script using the default parameters. The fragment mass spectra were searched against the Mus musculus SwissProt_2018_01 database (16965 entries) using Mascot (Matrix Science, London, UK; version 2.6.0) using the default probability cut-off score. The search variables that were used were: 10 ppm mass tolerance for precursor ion masses and 0.5 Da for product ion masses; digestion with trypsin; a maximum of two missed tryptic cleavages; variable modifications of oxidation of methionine and phosphorylation of serine, threonine, and tyrosine. Cross-correlation of Mascot search results with X! Tandem was accomplished with Scaffold (version Scaffold_4.8.7; Proteome Software, Portland, OR, USA). Probability assessment of peptide

assignments and protein identifications were made using Scaffold. Only peptides with ≥ 95% probability were considered.

Label-free peptide/protein quantification and identification.—Progenesis QI for proteomics software (version 2.4, Nonlinear Dynamics Ltd., Newcastle upon Tyne, UK) was used to perform ion-intensity based label-free quantification. In brief, in an automated format, .raw files were imported and converted into two-dimensional maps (y-axis =time, x-axis = m/z) followed by selection of a reference run for alignment purposes. An aggregate data set containing all peak information from all samples was created from the aligned runs, which was then further narrowed down by selecting only +2, +3, and + 4 charged ions for further analysis. The samples were then grouped and a peak list of fragment ion spectra from only the top eight most intense precursors of a feature was exported in Mascot generic file (.mgf) format and searched against the Mus musculus SwissProt_2018_01 database (16965 entries) using Mascot (Matrix Science, London, UK; version 2.4). The search variables that were used were: 10 ppm mass tolerance for precursor ion masses and 0.5 Da for product ion masses; digestion with trypsin; a maximum of two missed tryptic cleavages; variable modifications of oxidation of methionine and phosphorylation of serine, threonine, and tyrosine; 13C = 1. The resulting Mascot .xml file was then imported into Progenesis, allowing for peptide/protein assignment, while peptides with a Mascot Ion Score of < 25 were not considered for further analysis. Protein quantification was performed using only non-conflicting peptides and precursor ion-abundance values were normalized in a run to those in a reference run (not necessarily the same as the alignment reference run). Principal component analysis and unbiased hierarchal clustering analysis (heat map) was performed in Perseus (Tyanova et al., 2016; Tyanova and Cox, 2018) while Volcano plots were generated in RStudio.

4.12. Statistical power and data analysis

Experiments were performed to give 80% power to detect a treatment effect size of 20% compared to a baseline response of 5% at a significance level of 0.05 (Clayton and Collins, 2014; Andrews et al., 2015). Numbers required to achieve statistical power for each experiment were determined by G.Power3.1. Data analysis of Western blot was performed by quantifying the resultant bands using UN-SCAN-IT Gel 7.1 software. The NHE1 values were normalized to the determined α-tubulin levels. The data was graphed with statistics performed using GraphPad Prism 7 software. A repeated measure two-way analysis of variance (ANOVA) was used to analyze differences between treatment groups over time (i.e. TEER) with a Tukey's test applied post-hoc. All in vitro experiments were performed in duplicate in three individual trials. Unless otherwise stated, the data were expressed as mean ± SEM. Molecular studies were compared by one-way ANOVA or Student's T-test. When p-values were ≤ 0.05, they were accepted as statistically significant.

Supplementary Material

Refer to Web version on PubMed Central for supplementary material.

Funding

This work was supported by grants from the National Institute of Neurological Disorders and Stroke (R01NS099292, TML) of the National Institutes of Health, Arizona Biomedical Research Commission (ABRC45952, TML), with monies from the Department of Pharmacology at the University of Arizona and support from the Comprehensive Pain and Addiction Center (CPAC) at the University of Arizona College of Medicine Tucson. Authors are solely responsible for the content which does not necessarily represent the official views of the National Institutes of Health, the State of Arizona, or the University of Arizona.

Abbreviations:

BBB	blood brain barrier
E2	17-β-estradiol
NHE1	sodium-hydrogen exchanger 1
P	progesterone
T	testosterone
TEER	transendothelial resistance

7. Availability of Data and Material

The datasets used and/or analyzed during the current study are available from the corresponding author on reasonable request.

References

Abbott NJ, Patabendige AAK, Dolman DEM, Yusof SR, Begley DJ, 2010. Structure and function of the blood-brain barrier. Neurobiol. Dis. 37 (1), 13–25. 10.1016/j.nbd.2009.07.030. [PubMed: 19664713]

Amith SR, Vincent KM, Wilkinson JM, Postovit LM, Fliegel L, 2017. Defining the Na+/H+ exchanger NHE1 interactome in triple-negative breast cancer cells. Cell. Signal. 29, 69–77. 10.1016/j.cellsig.2016.10.005. [PubMed: 27751915]

Andrew RD, Hsieh Y-T, Brisson CD, 2017. Spreading depolarization triggered by elevated potassium is weak or absent in the rodent lower brain. J. Cereb. Blood. Flow. Metab. 37 (5), 1735–1747. 10.1177/0271678X16657344. [PubMed: 27381828]

Andrews NA, Latrémolière A, Basbaum AI, Mogil JS, Porreca F, Rice AS, Woolf CJ, Currie GL, Dworkin RH, Eisenach JC, et al. , 2015. Ensuring transparency and minimization of methodologic bias in preclinical pain research: PPRECISE considerations. Pain. 157, 901–909. 10.1097/j.pain.0000000000000458.

Atallah A, Mhaouty-Kodja S, Grange-Messent V, 2017. Chronic depletion of gonadal testosterone leads to blood-brain barrier dysfunction and inflammation in male mice. J. Cereb. Blood. Flow. Metab. 37 (9), 3161–3175. 10.1177/0271678X16683961. [PubMed: 28256950]

Avila M, Bansal A, Culberson J, Peiris AN, 2018. The Role of Sex Hormones in Multiple Sclerosis. Eur. Neurol. 80, 93–99. 10.1159/000494262. [PubMed: 30343306]

Ayata C, Lauritzen M, 2015. Spreading Depression, Spreading Depolarizations, and the Cerebral Vasculature. Physiol Rev. 95, 953–993. 10.1152/physrev.00027.2014. [PubMed: 26133935]

Azcoitia I, Barreto GE, Garcia-Segura LM, 2019. Molecular mechanisms and cellular events involved in the neuroprotective actions of estradiol. Analysis of sex differences. Front. Neuroendocrinol. 55, 100787 10.1016/j.yfrne.2019.100787. [PubMed: 31513774]

Basarsky TA, Feighan D, MacVicar BA, 1999. Glutamate release through volume-activated channels during spreading depression. J. Neurosci. 19, 6439–6445. 10.1523/JNEUROSCI.19-15-06439.1999. [PubMed: 10414972]

Beydoun R, Hamood MA, Gomez Zubieta DM, Kondapalli KC, 2017. Na+/H+ Exchanger 9 Regulates Iron Mobilization at the Blood-Brain Barrier in Response to Iron Starvation. J. Biol. Chem. 292, 4293–4301. 10.1074/jbc.M116.769240. [PubMed: 28130443]

Blaurock MC, Rebouças NA, Kusnezov JL, Igarashi P, 1995. Phylogenetically conserved sequences in the promoter of the rabbit sodium-hydrogen exchanger isoform 1 gene (NHE1/SLC9A1). Biochim. Biophys. Acta. 1262, 159–163. 10.1016/0167-4781(95)00075-r. [PubMed: 7599192]

Brennan KC, Beltrán-Parrazal L, López-Valdés HE, Theriot J, Toga AW, Charles AC, 2007a. Distinct vascular conduction with cortical spreading depression. J. Neurophysiol. 97, 4143–4151. 10.1152/jn.00028.2007. [PubMed: 17329631]

Brennan KC, Romero Reyes M, López Valdés HE, Arnold AP, Charles AC, 2007b. Reduced threshold for cortical spreading depression in female mice. Ann. Neurol. 61, 603–606. 10.1002/ana.21138. [PubMed: 17474110]

Brinton RD, 2008. The healthy cell bias of estrogen action: mitochondrial bioenergetics and neurological implications. Trends. Neurosci. 31, 529–537. 10.1016/j.tins.2008.07.003. [PubMed: 18774188]

Brinton RD, Thompson RF, Foy MR, Baudry M, Wang J, Finch CE, Morgan TE, Pike CJ, Mack WJ, Stanczyk FZ, Nilsen J, 2008. Progesterone receptors: form and function in brain. Front. Neuroendocrinol. 29, 313–339. 10.1016/j.yfrne.2008.02.001. [PubMed: 18374402]

Brzica H, Abdullahi W, Reilly BG, Ronaldson PT, 2018. Sex-specific differences in organic anion transporting polypeptide 1a4 (Oatp1a4) functional expression at the blood-brain barrier in Sprague-Dawley rats. Fluids Barriers CNS. 15, 25. 10.1186/s12987-018-0110-9. [PubMed: 30208928]

Bupha-Intr T, Wattanapermpool J, Peña JR, Wolska BM, Solaro RJ, 2007. Myofilament response to Ca2+ and Na+/H+ exchanger activity in sex hormone-related protection of cardiac myocytes from deactivation in hypercapnic acidosis. Am. J. Physiol. Regul. Integr. Comp. Physiol. 292, R837–843. 10.1152/ajpregu.00376.2006. [PubMed: 17038443]

Carraro-Lacroix LR, Ramirez MA, Zorn TM, Rebouças NA, Malnic G, 2006. Increased NHE1 expression is associated with serum deprivation-induced differentiation in immortalized rat proximal tubule cells. Am. J. Physiol. Renal. Physiol. 291, F129–139. 10.1152/ajprenal.00290.2005. [PubMed: 16495213]

Caruso D, Melis M, Fenu G, Giatti S, Romano S, Grimoldi M, Crippa D, Marrosu MG, Cavaletti G, Melcangi RC, 2014. Neuroactive steroid levels in plasma and cerebrospinal fluid of male multiple sclerosis patients. J. Neurochem. 130, 591–597. 10.1111/jnc.12745. [PubMed: 24766130]

Castañeda-Corral G, Rocha-González HI, Araiza-Saldaña CI, Vidal-Cantú GC, Miguel Jiménez-Andrade J, Murbartian J, Granados-Soto V, 2012. Blockade of peripheral and spinal Na+/H+ exchanger increases formalin-induced long-lasting mechanical allodynia and hyperalgesia in rats. Brain. Res. 1475, 19–30. 10.1016/j.brainres.2012.08.001. [PubMed: 22898152]

Chang CP, Wang SW, Huang ZL, Wang OY, Huang MI, Lu LM, Tarng DC, Chien CH, Chien EJ, 2010. Non-genomic rapid inhibition of Na+/H+-exchange 1 and apoptotic immunosuppression in human T cells by glucocorticoids. J. Cell. Physiol. 223, 679–686. 10.1002/jcp.22070. [PubMed: 20143335]

Charles AC, Baca SM, 2013. Cortical spreading depression and migraine. Nat. Rev. Neurol. 9, 637–644. 10.1038/nrneurol.2013.192. [PubMed: 24042483]

Chatterjee S, Schmidt S, Pouli S, Honisch S, Alkahtani S, Stournaras C, Lang F, 2014. Membrane androgen receptor sensitive Na+/H+ exchanger activity in prostate cancer cells. FEBS Lett. 588, 1571–1579. 10.1016/j.febslet.2014.02.040. [PubMed: 24607544]

Chien EJ, Liao CF, Chang CP, Pu HF, Lu LM, Shie MC, Hsieh DJ, Hsu MT, 2007. The non-genomic effects on Na+/H+-exchange 1 by progesterone and 20alpha-hydroxyprogesterone in human T cells. J. Cell. Physiol. 211, 544–550. 10.1002/jcp.20962. [PubMed: 17323380]

Chien EJ, Hsu CH, Chang VH, Lin EP, Kuo TP, Chien CH, Lin HY, 2016. In human T cells mifepristone antagonizes glucocorticoid non-genomic rapid responses in terms of Na(+)/H(+)-

exchange 1 activity, but not ezrin/radixin/moesin phosphorylation. Steroids. 111, 29–36. 10.1016/j.steroids.2016.01.004. [PubMed: 26773750]

Chung YC, Shin WH, Baek JY, Cho EJ, Baik HH, Kim SR, Won SY, Jin BK, 2016. CB2 receptor activation prevents glial-derived neurotoxic mediator production, BBB leakage and peripheral immune cell infiltration and rescues dopamine neurons in the MPTP model of Parkinson's disease. Exp. Mol. Med. 48, e205 10.1038/emm.2015.100. [PubMed: 27534533]

Clayton JA, Collins FS, 2014. Policy: NIH to balance sex in cell and animal studies. Nature. 509, 282–283. 10.1038/509282a. [PubMed: 24834516]

Cottier KE, Galloway EA, Calabrese EC, Tome ME, Liktor-Busa E, Kim J, Davis TP, Vanderah TW, Largent-Milnes TM, 2018. Loss of Blood-Brain Barrier Integrity in a KCl-Induced Model of Episodic Headache Enhances CNS Drug Delivery. eNeuro. 5, ENEURO.0116–18.2018. 10.1523/ENEURO.0116-18.2018.

Damkier HH, Christensen HL, Christensen IB, Wu Q, Fenton RA, Praetorius J, 2018. The murine choroid plexus epithelium expresses the 2Cl-/H+ exchanger ClC-7 and Na+/H+ exchanger NHE6 in the luminal membrane domain. Am. J. Physiol. Cell. Physiol. 314, C439–C448. 10.1152/ajpcell.00145.2017. [PubMed: 29351414]

Demaurex N, Orlowski J, Brisseau G, Woodside M, Grinstein S, 1995. The mammalian Na+/H+ antiporters NHE-1, NHE-2, and NHE-3 are electroneutral and voltage independent, but can couple to an H+ conductance. J. Gen. Physiol. 106, 85–111. 10.1085/jgp.106.1.85. [PubMed: 7494140]

Diler AS, Uzüm G, Akgün Dar K, Aksu U, Atukeren P, Ziylan YZ, 2007. Sex differences in modulating blood brain barrier permeability by NO in pentylenetetrazol-induced epileptic seizures. Life Sci. 80, 1274–1281. 10.1016/j.lfs.2006.12.039. [PubMed: 17306837]

Durham P, Papapetropoulos S, 2013. Biomarkers associated with migraine and their potential role in migraine management. Headache. 53, 1262–1277. 10.1111/head.12174. [PubMed: 23848170]

Fried NT, Maxwell CR, Elliott MB, Oshinsky ML, 2018. Region-specific disruption of the blood-brain barrier following repeated inflammatory dural stimulation in a rat model of chronic trigeminal allodynia. Cephalalgia. 38, 674–689. 10.1177/0333102417703764. [PubMed: 28457145]

Gholami K, Muniandy S, Salleh N, 2013. Differential expression of Na+/H+-exchanger (NHE-1, 2, and 4) proteins and mRNA in rodent's uterus under sex steroid effect and at different phases of the oestrous cycle. Biomed. Res. Int. 2013, 840121 10.1155/2013/840121. [PubMed: 23509787]

Gorodeski GI, Hopfer U, Liu CC, Margles E, 2005. Estrogen acidifies vaginal pH by up-regulation of proton secretion via the apical membrane of vaginal-ectocervical epithelial cells. Endocrinology. 146, 816–824. 10.1210/en.2004-1153. [PubMed: 15498880]

Gupta AK, Zygun DA, Johnston AJ, Steiner LA, Al-Rawi PG, Chatfield D, Shepherd E, Kirkpatrick PJ, Hutchinson PJ, Menon DK, 2004. Extracellular Brain pH and Outcome following Severe Traumatic Brain Injury. J. Neurotrauma. 21, 678–684. 10.1089/0897715041269722. [PubMed: 15253796]

Haim S, Shakhar G, Rossene E, Taylor AN, Ben-Eliyahu S, 2003. Serum levels of sex hormones and corticosterone throughout 4- and 5-day estrous cycles in Fischer 344 rats and their simulation in ovariectomized females. J. Endocrinol. Invest. 26, 1013–1022. 10.1007/BF03348201. [PubMed: 14759076]

Hartings JA, Shuttleworth CW, Kirov SA, Ayata C, Hinzman JM, Foreman B, Andrew RD, Boutelle MG, Brennan KC, Carlson AP, et al. , 2017. The continuum of spreading depolarizations in acute cortical lesion development: Examining Leão's legacy. J. Cereb. Blood. Flow. Metab. 37, 1571–1594. 10.1177/0271678X16654495. [PubMed: 27328690]

Hendus-Altenburger R, Kragelund BB, Pedersen SF, 2014. Structural dynamics and regulation of the mammalian SLC9A family of Na^+/H^+ exchangers. Curr. Top. Membr. 73, 69–148. 10.1016/B978-0-12-800223-0.00002-5. [PubMed: 24745981]

Hind WH, England TJ, O'Sullivan SE, 2016. Cannabidiol protects an in vitro model of the blood-brain barrier from oxygen-glucose deprivation via PPARγ and 5-HT1A receptors. Br. J. Pharmacol. 173, 815–825. 10.1111/bph.13368. [PubMed: 26497782]

Huang da W, Sherman BT, Lempicki RA, 2009. Systematic and integrative analysis of large gene lists using DAVID bioinformatics resources. Nat. Protoc. 4, 44–57. 10.1038/nprot.2008.211. [PubMed: 19131956]

Hun Lee J, Won S, Stein DG, 2015. Progesterone attenuates thrombin-induced endothelial barrier disruption in the brain endothelial cell line bEnd. 3: The role of tight junction proteins and the endothelial protein C receptor. Brain. Res. 1613, 73–80. 10.1016/j.brainres.2015.04.002. [PubMed: 25862570]

Ishrat T, Sayeed I, Atif F, Hua F, Stein DG, 2010. Progesterone and allopregnanolone attenuate blood-brain barrier dysfunction following permanent focal ischemia by regulating the expression of matrix metalloproteinases. Exp. Neurol. 226, 183–190. 10.1016/j.expneurol.2010.08.023. [PubMed: 20816826]

Jeong HJ, Chenu D, Johnson EE, Connor M, Vaughan CW, 2008. Sumatriptan inhibits synaptic transmission in the rat midbrain periaqueductal grey. Mol. Pain. 4, 54. 10.1186/1744-8069-4-54. [PubMed: 19014464]

Kilic A, Javadov S, Karmazyn M, 2009. Estrogen exerts concentration-dependent pro- and anti-hypertrophic effects on adult cultured ventricular myocytes. Role of NHE-1 in estrogen-induced hypertrophy. J. Mol. Cell Cardiol. 46, 360–369. 10.1016/j.yjmcc.2008.11.018. [PubMed: 19111554]

Kruse R, Krantz J, Barker N, Coletta RL, Rafikov R, Luo M, Højlund K, Mandarino LJ, Langlais PR, 2017. Characterization of the CLASP2 Protein Interaction Network Identifies SOGA1 as a Microtubule-Associated Protein. Mol. Cell. Proteomics. 16, 1718–1735. 10.1074/mcp.RA117.000011. [PubMed: 28550165]

Kuruca SE, Karadenizli S, Akgun-Dar K, Kapucu A, Kaptan Z, Uzum G, 2017. The effects of 17β-estradiol on blood brain barrier integrity in the absence of the estrogen receptor alpha; an in-vitro model. Acta. Histochem. 119, 638–647. 10.1016/j.acthis.2017.07.005. [PubMed: 28803749]

Lai JN, Wang OY, Lin VH, Liao CF, Tarng DC, Chien EJ, 2012. The non-genomic rapid acidification in peripheral T cells by progesterone depends on intracellular calcium increase and not on Na+/H+-exchange inhibition. Steroids. 77, 1017–1024. 10.1016/j.steroids.2012.03.004. [PubMed: 22449718]

Lam TI, Wise PM, O'Donnell ME, 2009. Cerebral microvascular endothelial cell Na/H exchange: evidence for the presence of NHE1 and NHE2 isoforms and regulation by arginine vasopressin. Am. J. Physiol. Cell. Physiol. 297, C278–289. 10.1152/ajpcell.00093.2009. [PubMed: 19458287]

Lam TI, Brennan-Minnella AM, Won SJ, Shen Y, Hefner C, Shi Y, Sun D, Swanson RA, 2013. Intracellular pH reduction prevents excitotoxic and ischemic neuronal death by inhibiting NADPH oxidase. Proc. Natl. Acad. Sci. U S A. 110, E4362–4368. 10.1073/pnas.1313029110. [PubMed: 24163350]

Lauritzen M, Dreier JP, Fabricius M, Hartings JA, Graf R, Strong AJ, 2011. Clinical relevance of cortical spreading depression in neurological disorders: migraine, malignant stroke, subarachnoid and intracranial hemorrhage, and traumatic brain injury. J. Cereb. Blood. Flow. Metab. 31, 17–35. 10.1038/jcbfm.2010.191. [PubMed: 21045864]

Li Z, Liu M, Lan L, Zeng F, Makris N, Liang Y, Guo T, Wu F, Gao Y, Dong M, Yang J, Li Y, Gong Q, Liang F, Kong J, 2016. Altered periaqueductal gray resting state functional connectivity in migraine and the modulation effect of treatment. Sci. Rep. 6, 20298. 10.1038/srep20298. [PubMed: 26839078]

Li L, Yun D, Zhang Y, Tao Y, Tan Q, Qiao F, Luo B, Liu Y, Fan R, Xian J, Yu A, 2018. A cannabinoid receptor 2 agonist reduces blood-brain barrier damage via induction of MKP-1 after intracerebral hemorrhage in rats. Brain Res. 1697, 113–123. 10.1016/j.brainres.2018.06.006. [PubMed: 29886251]

Liktor-Busa E, Blawn KT, Kellohen KL, Wiese BM, Verkhovsky V, Wahl J, Vivek A, Palomino SM, Davis TP, Vanderah TW, Largent-Milnes TM, 2020. Functional NHE1 expression is critical to blood brain barrier integrity and sumatriptan blood to brain uptake. PLoS One. 15, e0227463 10.1371/journal.pone.0227463. [PubMed: 32469979]

Limmroth V, Lee WS, Moskowitz MA, 1996. GABAA-receptor-mediated effects of progesterone, its ring-A-reduced metabolites and synthetic neuroactive steroids on neurogenic oedema in the rat meninges. Br. J. Pharmacol. 117, 99–104. 10.1111/j.1476-5381.1996.tb15160.x. [PubMed: 8825349]

Lin Z, Reierstad S, Huang CC, Bulun SE, 2007. Novel estrogen receptor-alpha binding sites and estradiol target genes identified by chromatin immunoprecipitation cloning in breast cancer. Cancer Res. 67, 5017–5024. 10.1158/0008-5472.CAN-06-3696. [PubMed: 17510434]

Lin X, Kraut JA, Wu D, 2014. Coadministration of a Na+-H+ exchange inhibitor and sodium bicarbonate for the treatment of asphyxia-induced cardiac arrest in piglets. Pediatr. Res. 76, 118–126. 10.1038/pr.2014.65. [PubMed: 24796369]

Luo J, Kintner DB, Shull GE, Sun D, 2007. ERK1/2-p90RSK-mediated phosphorylation of Na+/H+ exchanger isoform 1. A role in ischemic neuronal death. J. Biol. Chem. 282, 28274–28284. 10.1074/jbc.M702373200. [PubMed: 17664275]

Maggioli E, McArthur S, Mauro C, Kieswich J, Kusters DHM, Reutelingsperger CPM, Yaqoob M, Solito E, 2016. Estrogen protects the blood-brain barrier from inflammation-induced disruption and increased lymphocyte trafficking. Brain. Behav. Immun. 51, 212–222. 10.1016/j.bbi.2015.08.020. [PubMed: 26321046]

Masereel B, Pochet L, Laeckmann D, 2003. An overview of inhibitors of Na(+)/H(+) exchanger. Eur. J. Med. Chem. 38, 547–554. 10.1016/s0223-5234(03)00100-4. [PubMed: 12832126]

Mathew NT, 2011. Pathophysiology of chronic migraine and mode of action of preventive medications. Headache. 51 (Suppl 2), 84–92. 10.1111/j.1526-4610.2011.01955.x. [PubMed: 21770930]

Milosavljevic N, Monet M, Léna I, Brau F, Lacas-Gervais S, Feliciangeli S, Counillon L, Poët M, 2014. The intracellular Na(¨ +)/H(+) exchanger NHE7 effects a Na(+)-coupled, but not K(+)-coupled proton-loading mechanism in endocytosis. Cell. Rep. 7, 689–696. 10.1016/j.celrep.2014.03.054. [PubMed: 24767989]

Na W, Lee JY, Kim WS, Yune TY, Ju BG, 2015. 17beta-Estradiol Ameliorates Tight Junction Disruption via Repression of MMP Transcription. Mol. Endocrinol. 29, 1347–1361. 10.1210/ME.2015-1124. [PubMed: 26168035]

Naguib S, Ahmad V, Kasim N, Amri S, Onn Y, 2011. The effect of progesterone on uterine fluid ph & endometrial nhe-1 protein expression in rats. Health. 3, 66–72. 10.4236/health.2011.31012.

Nierwińska K, Nowacka-Chmielewska M, Bernacki J, Jagsz S, Chalimoniuk M, Langfort J, Małecki A, 2019. The effect of endurance training and testosterone supplementation on the expression of blood spinal cord barrier proteins in rats. PLoS One. 14, e0211818 10.1371/journal.pone.0211818.

Nørholm AB, Hendus-Altenburger R, Bjerre G, Kjaergaard M, Pedersen SF, Kragelund BB, 2011. The intracellular distal tail of the Na+/H+ exchanger NHE1 is intrinsically disordered: implications for NHE1 trafficking. Biochemistry. 50, 3469–3480. 10.1021/bi1019989. [PubMed: 21425832]

O'Donnell ME, 2014. Blood-brain barrier Na transporters in ischemic stroke. Adv. Pharmacol. 71, 113–146. 10.1016/bs.apha.2014.06.011. [PubMed: 25307215]

Parker SS, Krantz J, Kwak EA, Barker NK, Deer CG, Lee NY, Mouneimne G, Langlais PR, 2019. Insulin Induces Microtubule Stabilization and Regulates the Microtubule Plus-end Tracking Protein Network in Adipocytes. Mol. Cell. Proteomics. 18, 1363–1381. 10.1074/mcp.RA119.001450. [PubMed: 31018989]

Pietrobon D, Moskowitz MA, 2014. Chaos and commotion in the wake of cortical spreading depression and spreading depolarizations. Nat. Rev. Neurosci. 15, 379–393. 10.1038/nrn3770. [PubMed: 24857965]

Plackett TP, Deburghraeve CR, Palmer JL, Gamelli RL, Kovacs EJ, 2016. Effects of Estrogen on Bacterial Clearance and Neutrophil Response After Combined Burn Injury and Wound Infection. J. Burn. Care. Res. 37, 328–333. 10.1097/BCR.0000000000000340. [PubMed: 27058581]

Prasad H, Rao R, 2015. The Na+/H+ exchanger NHE6 modulates endosomal pH to control processing of amyloid precursor protein in a cell culture model of Alzheimer disease. J. Biol. Chem. 290, 5311–5327. 10.1074/jbc.M114.602219. [PubMed: 25561733]

Putney LK, Denker SP, Barber DL, 2002. The changing face of the Na+/H+ exchanger, NHE1: structure, regulation, and cellular actions. Annu. Rev. Pharmacol. Toxicol. 42, 527–552. 10.1146/annurev.pharmtox.42.092001.143801. [PubMed: 11807182]

Qadri SM, Su Y, Cayabyab FS, Liu L, 2014. Endothelial Na+/H+ exchanger NHE1 participates in redox-sensitive leukocyte recruitment triggered by methylglyoxal. Cardiovasc. Diabetol. 13, 134. 10.1186/s12933-014-0134-7. [PubMed: 25270604]

Rajkumar L, Guzman RC, Yang J, Thordarson G, Talamantes F, Nandi S, 2001. Short-term exposure to pregnancy levels of estrogen prevents mammary carcinogenesis. Proc. Natl. Acad. Sci. U S A. 98, 11755–11759. 10.1073/pnas.201393798. [PubMed: 11573010]

Russo AF, 2015. Calcitonin gene-related peptide (CGRP): a new target for migraine. Annu. Rev. Pharmacol. Toxicol. 55, 533–552. 10.1146/annurev-pharmtox-010814-124701. [PubMed: 25340934]

Sárvári M, Kalló I, Hrabovszky E, Solymosi N, Rodolosse A, Liposits Z, 2016. Long-Term Estrogen Receptor Beta Agonist Treatment Modifies the Hippocampal Transcriptome in Middle-Aged Ovariectomized Rats. Front. Cell. Neurosci. 10, 149. 10.3389/fncel.2016.00149. [PubMed: 27375434]

Schipper HM, 1986. Neurology of sex steroids and oral contraceptives. Neurol. Clin. 4, 721–751. [PubMed: 3025581]

Seillet C, Rouquié N, Foulon E, Douin-Echinard V, Krust A, Chambon P, Arnal JF, Guéry JC, Laffont S, 2013. Estradiol promotes functional responses in inflammatory and steady-state dendritic cells through differential requirement for activation function-1 of estrogen receptor α. J. Immunol. 190, 5459–5470. 10.4049/jimmunol.1203312. [PubMed: 23626011]

Shi Y, Chanana V, Watters JJ, Ferrazzano P, Sun D, 2011. Role of sodium/hydrogen exchanger isoform 1 in microglial activation and proinflammatory responses in ischemic brains. J. Neurochem. 119, 124–135. 10.1111/j.1471-4159.2011.07403.x. [PubMed: 21797866]

Shi Y, Kim D, Caldwell M, Sun D, 2013. The role of Na(+)/h (+) exchanger isoform 1 in inflammatory responses: maintaining H(+) homeostasis of immune cells. Adv. Exp. Med. Biol. 961, 411–418. 10.1007/978-1-4614-4756-6_35. [PubMed: 23224899]

Si D, Li J, Liu J, Wang X, Wei Z, Tian Q, Wang H, Liu G, 2014. Progesterone protects blood-brain barrier function and improves neurological outcome following traumatic brain injury in rats. Exp. Ther. Med. 8, 1010–1014. 10.3892/etm.2014.1840. [PubMed: 25120639]

Singh Y, Zhou Y, Shi X, Zhang S, Umbach AT, Salker MS, Lang KS, Lang F, 2016. Alkaline Cytosolic pH and High Sodium Hydrogen Exchanger 1 (NHE1) Activity in Th9 Cells. J. Biol. Chem. 291, 23662–23671. 10.1074/jbc.M116.730259. [PubMed: 27629415]

Song S, Wang S, Pigott VM, Jiang T, Foley LM, Mishra A, Nayak R, Zhu W, Begum G, Shi Y, Carney KE, Hitchens TK, Shull GE, Sun D, 2018. Selective role of Na+ /H+ exchanger in Cx3cr1+ microglial activation, white matter demyelination, and post-stroke function recovery. Glia. 66, 2279–2298. 10.1002/glia.23456. [PubMed: 30043461]

Sun X, Wang Y, Chen S, Luo W, Li P, Luo Q, 2011. Simultaneous monitoring of intracellular pH changes and hemodynamic response during cortical spreading depression by fluorescence-corrected multimodal optical imaging. Neuroimage. 57, 873–884. 10.1016/j.neuroimage.2011.05.040. [PubMed: 21624475]

Tomás-Camardiel M, Venero JL, Herrera AJ, De Pablos RM, Pintor-Toro JA, Machado A, Cano J, 2005. Blood-brain barrier disruption highly induces aquaporin-4 mRNA and protein in perivascular and parenchymal astrocytes: protective effect by estradiol treatment in ovariectomized animals. J. Neurosci. Res. 80, 235–246. 10.1002/jnr.20443. [PubMed: 15772982]

Torres L, Bynoe MS, 2017. Influence of gender on blood brain barrier permeability and adenosine receptor signaling. FASEB J. 31, 1042.3–1042.3. doi.10.1096/fasebj.31.1_supplement.1042.3.

Turovsky E, Theparambil SM, Kasymov V, Deitmer JW, Del Arroyo AG, Ackland GL, Corneveaux JJ, Allen AN, Huentelman MJ, Kasparov S, Marina N, Gourine AV, 2016. Mechanisms of CO2/H+ Sensitivity of Astrocytes. J. Neurosci. 36, 10750–10758. 10.1523/JNEUROSCI.1281-16.2016. [PubMed: 27798130]

Tyanova S, Cox J, 2018. Perseus: A Bioinformatics Platform for Integrative Analysis of Proteomics Data in Cancer Research. Methods. Mol. Biol. 1711, 133–148. 10.1007/978-1-4939-7493-1_7. [PubMed: 29344888]

Tyanova S, Temu T, Sinitcyn P, Carlson A, Hein MY, Geiger T, Mann M, Cox J, 2016. The Perseus computational platform for comprehensive analysis of (prote) omics data. Nat. Methods. 13, 731–740. 10.1038/nmeth.3901. [PubMed: 27348712]

Vallés PG, Bocanegra V, Gil Lorenzo A, Costantino VV, 2015. Physiological Functions and Regulation of the Na+/H+ Exchanger [NHE1] in Renal Tubule Epithelial Cells. Kidney. Blood. Press. Res. 40, 452–466. 10.1159/000368521. [PubMed: 26304834]

Wang XF, Yu MK, Lam SY, Leung KM, Jiang JL, Leung PS, Ko WH, Leung PY, Chew SB, Liu CQ, Tse CM, Chan HC, 2003. Expression, immunolocalization, and functional activity of Na+/H+ exchanger isoforms in mouse endometrial epithelium. Biol. Reprod. 68, 302–308. 10.1095/biolreprod.102.005645. [PubMed: 12493726]

Wang Z, Li Y, Cai S, Li R, Cao G, 2018. Cannabinoid receptor 2 agonist attenuates blood-brain barrier damage in a rat model of intracerebral hemorrhage by activating the Rac1 pathway. Int. J. Mol. Med. 42, 2914–2922. 10.3892/ijmm.2018.3834. [PubMed: 30132506]

Wizemann TM, Pardue ML, 2001. Exploring the Biological Contributions to Human Health: Does Sex Matter?, first ed. National Academies Press, Washington (DC).

Xiao H, Deng M, Yang B, Hu Z, Tang J, 2018. Pretreatment with 17β-Estradiol attenuates cerebral ischemia-induced blood-brain barrier disruption in aged rats: involvement of antioxidant signaling. Neuroendocrinology. 106, 20–29. 10.1159/000455866. [PubMed: 28196366]

Yuen NY, Chechneva OV, Chen YJ, Tsai YC, Little LK, Dang J, Tancredi DJ, Conston J, Anderson SE, O'Donnell ME, 2018. Exacerbated brain edema in a rat streptozotocin model of hyperglycemic ischemic stroke: Evidence for involvement of blood-brain barrier Na-K-Cl cotransport and Na/H exchange. J. Cereb. Blood. Flow. Metab. 39, 1678–1692. 10.1177/0271678X18770844. [PubMed: 29739261]

Zárate S, Stevnsner T, Gredilla R, 2017. Role of estrogen and other sex hormones in brain aging. Neuroprotection and DNA Repair. Front. Aging. Neurosci. 9, 430. 10.3389/fnagi.2017.00430. [PubMed: 29311911]

Zaun HC, Shrier A, Orlowski J, 2012. N-myristoylation and Ca2+ binding of calcineurin B homologous protein CHP3 are required to enhance Na+/H+ exchanger NHE1 half-life and activity at the plasma membrane. J. Biol. Chem. 287, 36883–36895. 10.1074/jbc.M112.394700. [PubMed: 22984264]

Zhao H, Carney KE, Falgoust L, Pan JW, Sun D, Zhang Z, 2016. Emerging roles of Na^+/H^+ exchangers in epilepsy and developmental brain disorders. Prog. Neurobiol. 138–140, 19–35. 10.1016/j.pneurobio.2016.02.002.

Zhou C, Baltz JM, 2013. JAK2 mediates the acute response to decreased cell volume in mouse preimplantation embryos by activating NHE1. J. Cell. Physiol. 228, 428–438. 10.1002/jcp.24147. [PubMed: 22740348]

Zohsel K, Hohmeister J, Oelkers-Ax R, Flor H, Hermann C, 2006. Quantitative sensory testing in children with migraine: preliminary evidence for enhanced sensitivity to painful stimuli especially in girls. Pain. 123, 10–18. 10.1016/j.pain.2005.12.015. [PubMed: 16495010]

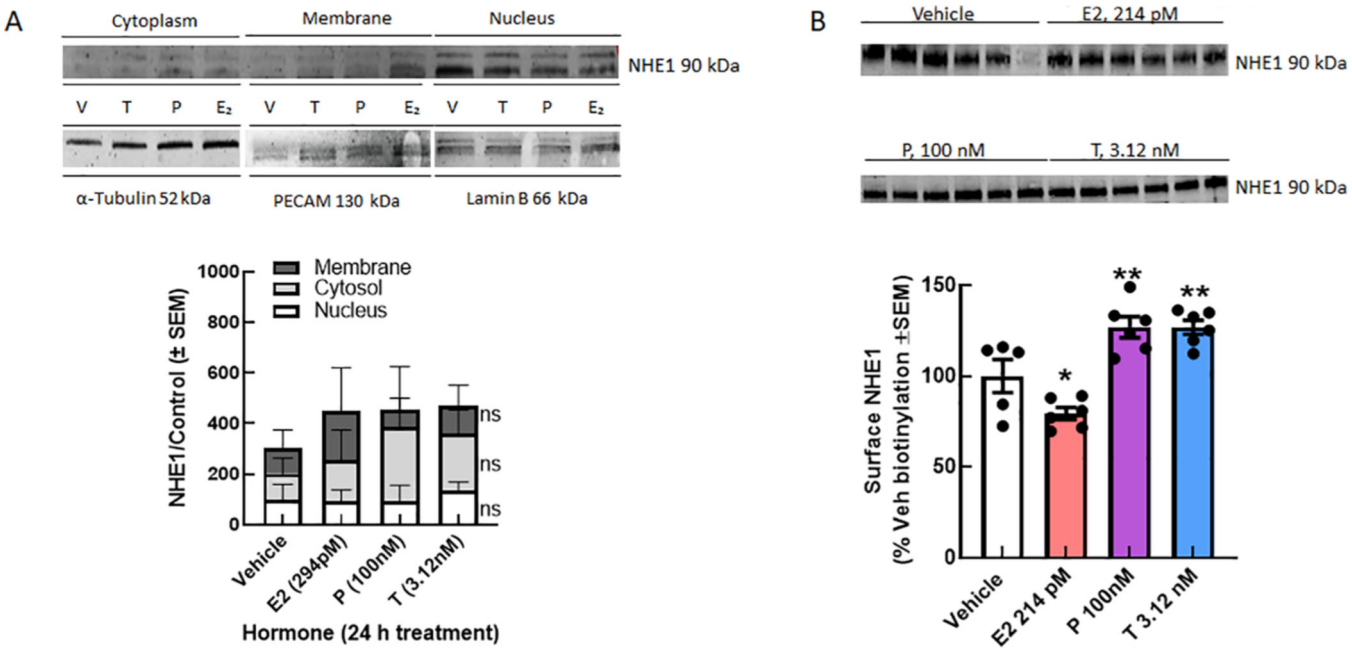

Fig. 1.

Progesterone and Testosterone, but not E2, increase cell surface expression of NHE1. A. Total expression of NHE1 in immortalized bEnd.3 cells is unchanged by 24 h hormone exposure. B. Subcellular fractionation shows no statistical difference in the detection of NHE1 in membrane, cytosolic, or nuclear fractions after hormone exposure. C. Biotinylation pulldown of bEnd.3 mouse brain endothelial cells showed that 24 h exposure to E2 (294 pM) significantly decreased cell surface expression of NHE1, whereas T (3.12 nM) and P (100 nM) significantly increased cell surface expression of NHE1 as compared to vehicle. N = 3–4 individual experiments in triplicate. One-way ANOVA $F(3,19) = 17.65$, $p < 0.001$, Dunnett post-hoc *$p < 0.05$, ** $p < 0.01$.

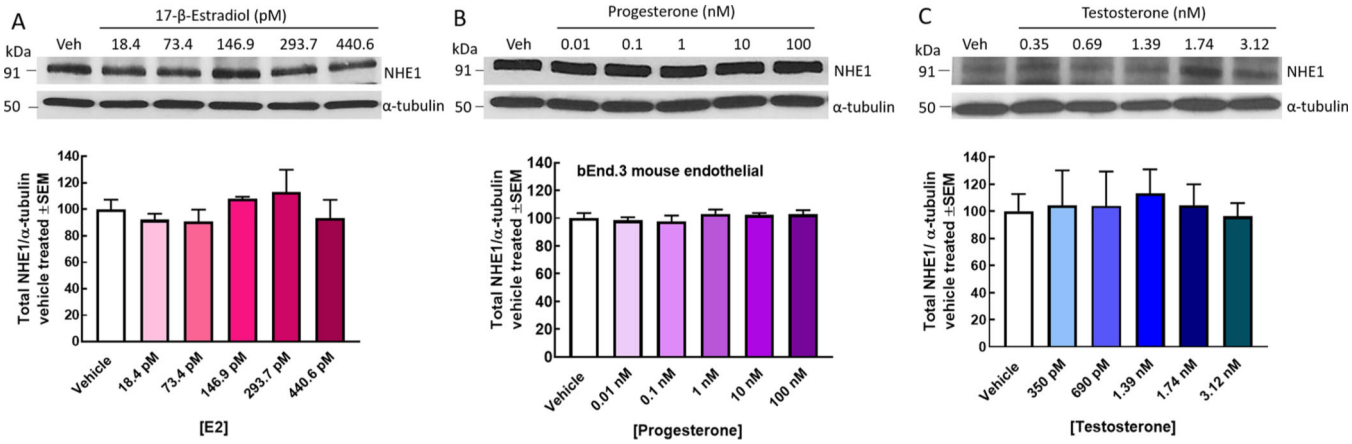

Fig. 2.

Sex hormones do not change total NHE1 expression. bEnd.3 endothelial cells treated for 24 h with (A) E2, (B) P, or (C) T did not show a change in NHE1 total expression across the physiological range of concentrations. N = 3–4 individual experiments in triplicate.

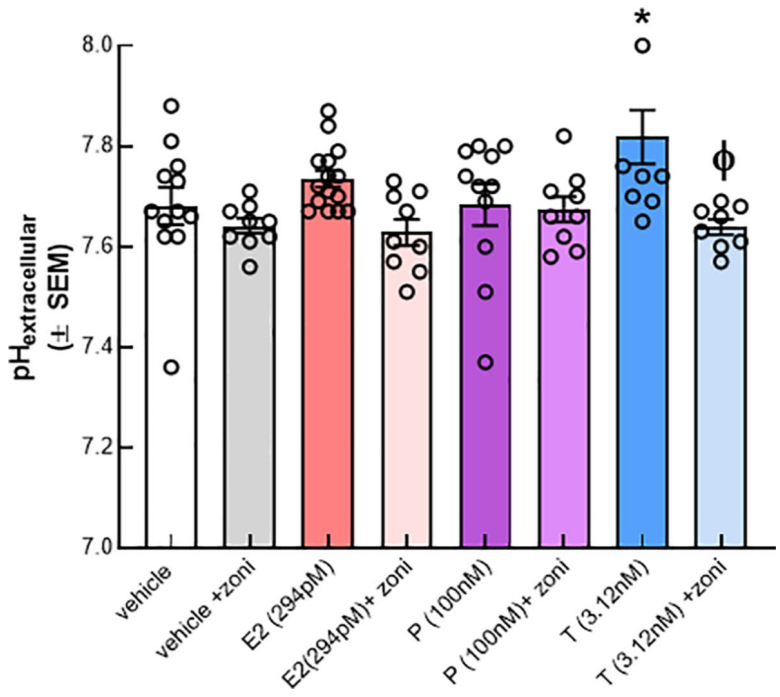

Fig. 3.

T, but not E2 or P, increases extracellular pH (pHe) following 24 h exposure. pHe was measured after a 24 incubation with E2 (294 pM), P (100 nm), and T (3.12 nM); dark bars. Neither E2 nor P resulted in a changed pHe. Testosterone significantly increase the pHe (media pH) as compared to vehicle. This could be blocked by the NHE1 inhibitor, zoniporide (10 nM; light bars). N = 3–4 individual experiments in triplicate. One-way ANOVA $F(7,74) = 3.61$, $p < 0.001$, Bonferroni post-hoc*$p < 0.05$ vs. vehicle, $^{\phi}p < 0.05$, Testosterone vs T + zoniporide.

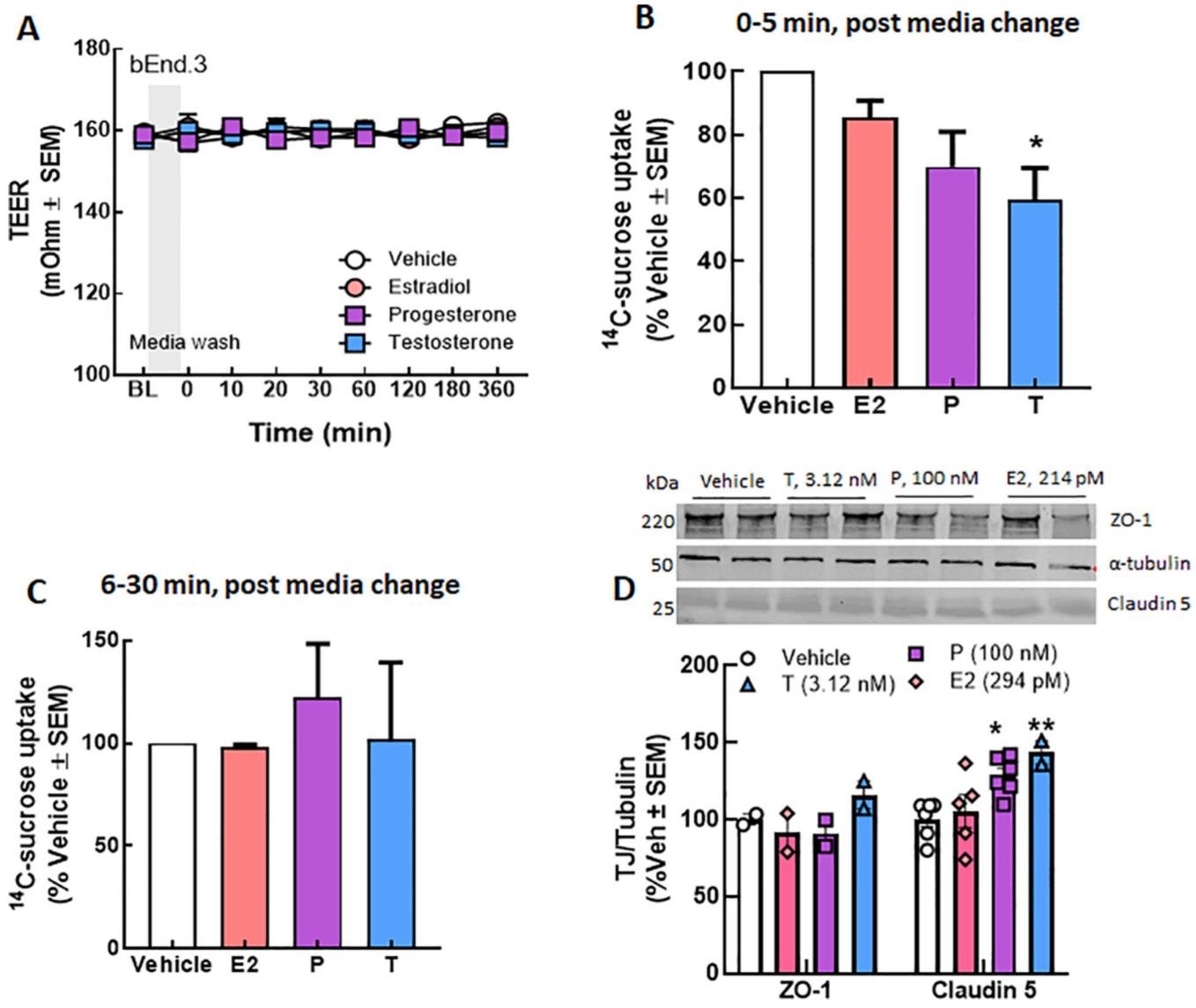

Fig. 4.

Hormone regulation of brain endothelial cell basal paracellular integrity. (A) TEER values are unchanged following 24 h exposure to E2, P, and T as compared to vehicle treatment. (B) ^{14}Csucrose passage is reduced beyond that of vehicle after incubation with T and a short media wash period that was not attributed to cell confluency. Sucrose movement normalizes after 30 min (C). Differences in functional monolayer integrity could be attributed to differences in the tight junction expression following exposure to individual hormones. Two-way ANOVA ZO1: $F(3,19) = 3.921$, Tukey post-hoc, $p = 0.01–0.03$.

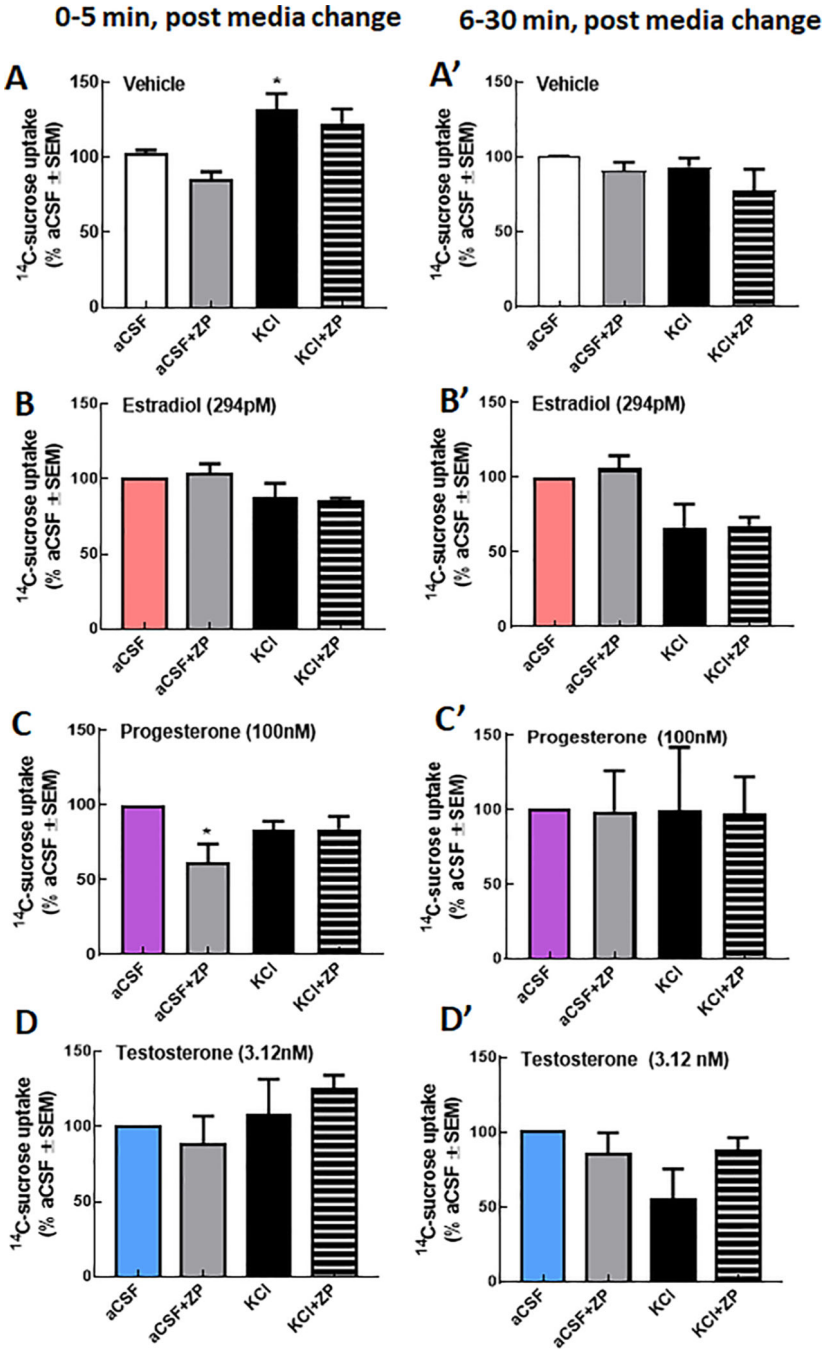

Fig. 5.

Progesterone, but not E2 or T, regulation of KCl induced paracellular breaches require NHE1. Paracellular integrity of the bEnd.3 monolayer was assessed using passage of ^{14}C-sucrose from the luminal to abluminal side of *trans*-well inserts. KCl (60 mM, 5 min) significantly enhance ^{14}C-sucrose movement after (A, A') vehicle but not E2 (B, B'), P (C, C') or T (D, D'). One-way ANOVA $F(3,8) = 8.92$, $p = 0.0008$, Bonferroni post-hoc*$p < 0.05$ vs. aCSF. Progesterone (D) sensitized bEND.3 cells to zoniporide in aCSF pulsed conditions leading to a significant reduction in ^{14}C-sucrose movement. One-way ANOVA $F(3, 8) =$

8.92, p = 0.05, Bonferroni post-hoc*p <0.05 vs. aCSF. N = 3–4 individual experiments in triplicate.

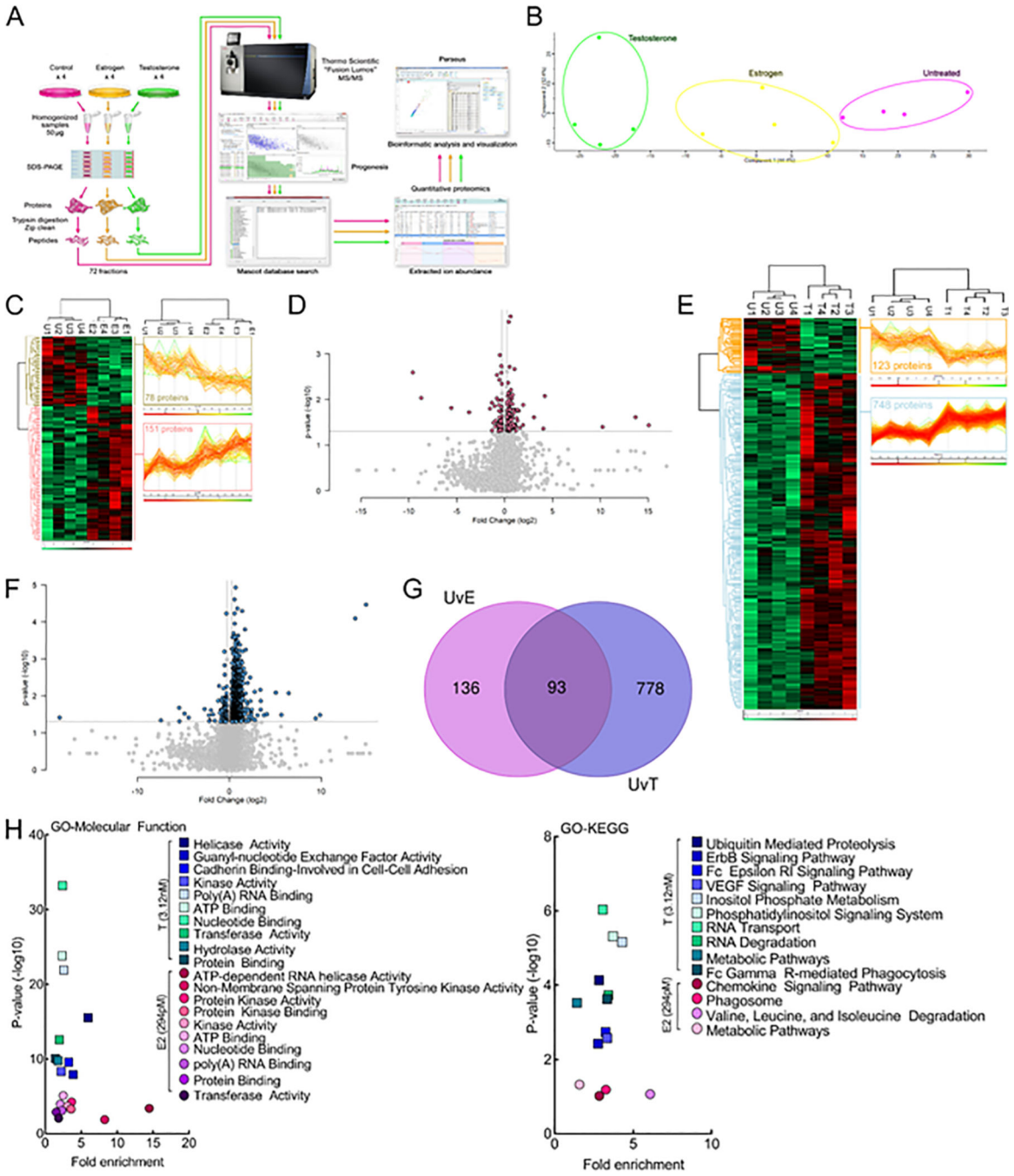

Fig. 6.

Proteomic analysis of bEnd.3 endothelial cells reveals differences in hormone-regulated molecular function and KEGG pathways.17-β-Estradiol and testosterone differentially regulate the protein expression levels of bEnd.3 endothelial cells in vitro. (A) Schematic diagram of the label-free quantitative proteomics experimental approach (n = 4). bEnd.3 endothelial cells were treated and lysed as described in Materials & Methods. 200 μg of lysate was separated by 10% SDS-PAGE and each gel lane was fractionated into six gel slices that were subjected to trypsin digestion. The resulting tryptic digest was

purified and subsequently analyzed by tandem mass spectrometry. Raw data processing for quantification was executed in Progenesis QI for Proteomics and peptide/protein identification was performed by database searching with Mascot. The resulting Mascot peptide and protein identifications were imported into Progenesis QI for Proteomics and quantification of changes in peptide/protein abundance was performed via extracted ion abundance in Progenesis QI for Proteomics. The resulting quantitative proteomics data was further processed by Perseus for visual representation of the findings. MS/MS, tandem mass spectrometry. (B) Unbiased principal component analysis (PCA) of the 805 significantly affected proteins from the 3-way ANOVA analysis of the quantitative proteomics data revealed that the protein expression differences of the individual biological samples within each group were consistent and no outliers were detected and also indicated that testosterone had a more significant effect on protein expression versus estrogen (relative to the untreated control). (C) Unbiased hierarchical clustering of the 229 significantly affected proteins in the estrogen versus untreated control treatment groups confirmed that the expression patterns across the different individual biological samples cluster together accordingly as either untreated control or estrogen. A heat map and linked dendrogram of the hierarchical clustering results provide a visual representation of the clustered matrix and the associated profile plots further reveal consistency within groups of the corresponding protein expression patterns (see the two boxes to the right of the heat map). (D) A volcano plot of the estrogen versus untreated control. Above the horizontal grey line represents the cut-off for a p value of <0.5 while the two vertical lines represent the cut-off values of 1.2-fold change in either the positive or negative direction. (E) Unbiased hierarchical clustering of the 871 significantly affected proteins in the testosterone versus untreated control treatment groups confirmed that the expression patterns across the different individual biological samples cluster together accordingly as either untreated control or testosterone. A heat map and linked dendrogram of the hierarchical clustering results provide a visual representation of the clustered matrix and the associated profile plots further reveal consistency within groups of the corresponding protein expression patterns (see the two boxes to the right of the heat map). (F) A volcano plot of the testosterone versus untreated control. Above the horizontal grey line represents the cut-off for a p value of <0.5 while the two vertical lines represent the cut-off values of 1.2-fold change in either the positive or negative direction. (G) A Venn diagram of the significantly affected proteins in the untreated control versus estrogen (UvE) experiment compared to the untreated control versus testosterone (UvT) experiment. (H) Scatter plots of the “Molecular Function” and “KEGG pathways” gene ontology enrichment findings for both the untreated control versus estrogen and untreated control versus testosterone experiments. GO, gene ontology. N = 4/treatment.

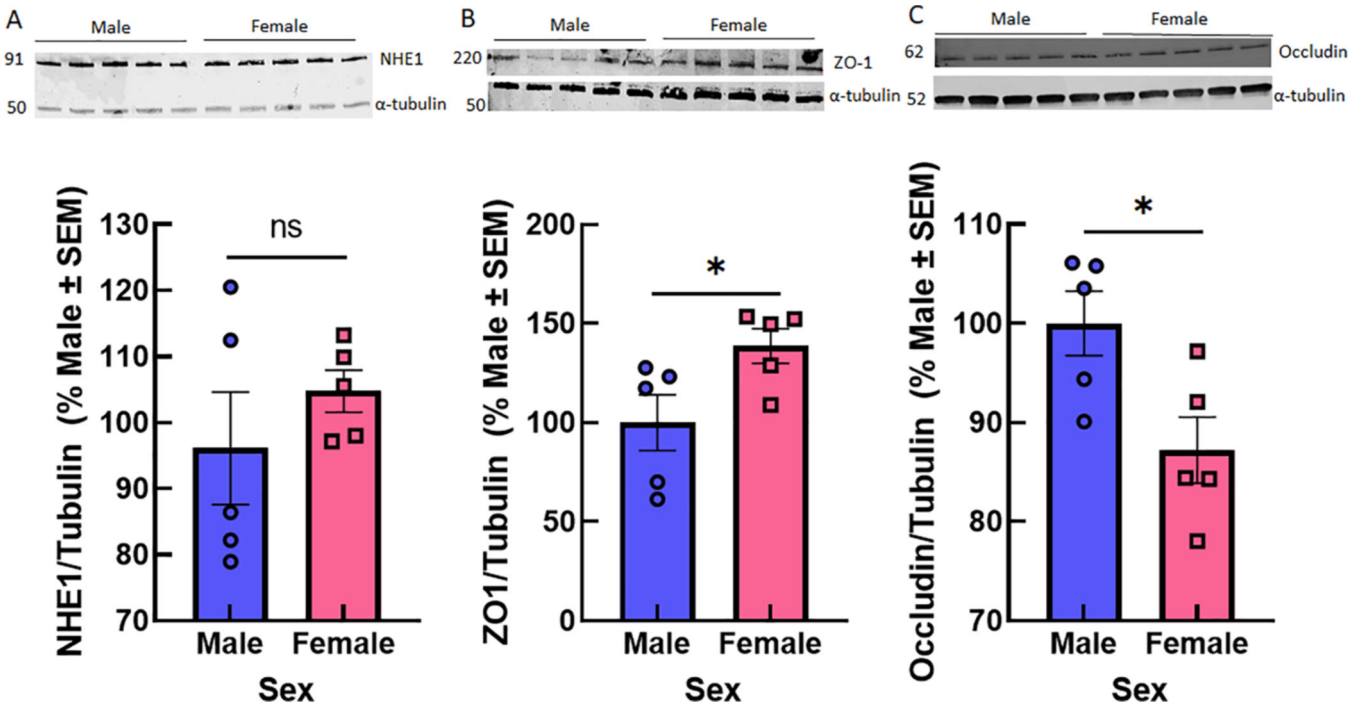

Fig. 7.

NHE1 and ZO-1 expression from cortical samples of male and female CD1 mice. (A) NHE1 did not show statistical differences in total expression in whole samples of brain tissue from male and female CD1 mice. (B) Zo-1 and (C) Occludin were statistically different between the sexes (n = 5/sex). Unpaired T-test NHE1: p = 0.37; ZO-1: p = 0.048; Occludin p = 0.026 *p < 0.05.